

**Marina Solé Espeso**

**Synthesis of a New Hole Transporting Material and its Application in  
Perovskites Solar Cells**

**TREBALL DE FI DE GRAU**

**dirigit pel Dr. Emilio Palomares**

**Grau de Química**



**UNIVERSITAT ROVIRA I VIRGILI**

**Tarragona**

**2015**



## Resum

Actualment, el subministrament de més del 80% de l'energia generada a tot el món prové de fonts no renovables, sovint localitzades en punts concrets del territori i fortament contaminants. El problema de sostenibilitat i de contaminació que suposa la seva vasta explotació és una de les principals preocupacions avui en dia. D'aquesta manera, l'aprofitament d'altres energies, més netes, renovables i accessibles, ha passat a ser un punt clau per al manteniment del nostre nivell de vida i pel creixement econòmic de la nostra economia.

Una de les fonts d'energia no finites més estudiades és la solar. La optimització en mètodes de recollida, emmagatzematge i aprofitament d'aquesta energia és un tema d'investigació candent, i ja ha proporcionat la fabricació i comercialització de dispositius relativament eficients. Per tal d'augmentar-ne l'eficiència, i poder fer que els seus preus de mercat competeixin amb els de les energies no renovables, aquesta investigació és altament necessària.

En aquest treball es fa una petita aportació a aquesta investigació, sintetitzant una nova molècula per tal d'optimitzar una de les parts de cel·les solars de perovskites, un tipus de dispositius molt nous i prometedors. El treball inclou un breu fonament teòric del funcionament d'aquestes cel·les i com caracteritzar-les, una part experimental on es descriu la síntesi de la molècula objectiu i la fabricació dels dispositius, i finalment una explicació dels resultats obtinguts.

# Contents

Introduction.....	5
1. Global Energy.....	5
2. Collecting the sun's energy: photovoltaic solar cells.....	6
Objectives.....	8
Fundamentals of Perovskites Solar Cells.....	9
1. Photovoltaic Systems.....	9
2. Overview of electrical properties of a semiconductor.....	9
3. Perovskites solar cells: main components.....	10
4. Operation of perovskites solar cells.....	12
5. Solar cells characterization.....	13
6. Synthesis of a nobel indoline derivate HTM.....	16
Experimental Section.....	17
1. Table of reactivities.....	17
2. Synthesis of ML01.....	24
3. Device Fabrication.....	29
4. Device Characterization.....	34
Results and Discussion.....	35
1. Synthesis of ML01.....	35
2. Device characterization.....	44
Conclusions.....	46
Bibliography.....	47

# Introduction

## 1. Energy

Nowadays, more than 80% of the global energy used comes from fossil fuels because of the huge amount of energy released in their combustion. Fossil fuels are organic matter created by natural decomposition of organic matter over many years. The most common examples are coal, oil and natural gas.

As they require so many years to be created, they are a type of energy depletable, known as non-renewable energy. The fact that they cannot be regenerated and their huge actual exploitation presents an important sustainability problem.

Moreover, though some of them can be found in many parts of the territory, some other fossil fuels are concentrated in specific areas, which means in particular countries, so their global use has to overcome political and economic barriers.

On top of that, their combustion is one of the first causes of serious environmental problems, because it produces many gases that contribute to acid rain, smog, greenhouse effect or ozone depletion. Recollection, process and distribution of these fossil fuels can also provide contaminating or environmental problems.

The problematic of these combustibles lead to the study of new and cleaner sources of energy and with the ability to regenerate themselves, the known as renewable energies. Among these group of sources, wind, hydro and solar energy are the most important.

Solar energy, in comparison with the other renewables energies, is not limited by the territory features, because the solar source covers the whole world, not depending by aquatic or windy zone conditions. Furthermore, solar energy devices can be installed in existing buildings in aesthetic manner, and do not need to occupy nor change large areas of landscape. Consequently, solar energy is the renewable energy that brings the less environmental impact<sup>1</sup>.

Concerning to the economy, the devices fabrication and installation used in hydroelectric energy are the most expensive, followed by the wind turbines. Thus, solar energy devices are in principle the most cost effective ones<sup>1</sup>.

Nevertheless, renewable energy collection is nowadays much less economic and efficient than that obtained from fossil fuels. Is for that reason that there is a major need of optimize methods

and devices to obtain and use energy from renewable sources in a much more cheaper and efficient way.

## 2. Collecting the sun's energy: photovoltaic solar cells

Photovoltaic solar cells are devices that produce electricity when exposed to sunlight. The first knowledge related with this subject came out in 1839, when the French scientist Adam Becquerél reported the first photovoltaic effect and explained how electricity could be generated from sun. His experiments were based on using two silver electrodes submerged in an electrolytic conducting solution, so when the cell was submitted to sunlight, a current flow was generated<sup>2</sup>.

Later in 1876, William G. Adams and Richard E. Day discovered that sunlight applied to a solid selenium wire could produce electricity. However, solar cells precursors developed subsequently had not enough conversion efficiency to be commercialized<sup>2</sup>.

Almost 100 hundred years later and with all the investigation about photovoltaics, in 1954 Bell Labs' scientists developed the first silicon photovoltaic cell, which gave a greater current than selenium wire when exposed to sunlight. Thereafter, solar cells investigation became of great interest<sup>2</sup>.

Since they appeared until nowadays, the knowledge about solar cells is wide and investigation on how to optimize them is a hot topic. Nowadays, solar cells can be divided into 3 generations depending on the material and the processing technology used to fabricate them:

The first generation consists basically on silicon-based cells made of semiconducting p-n junctions. Since they were the first in appear, they are the most improved and the most commercialized, and they show good efficiencies, reaching the maximum of 27.6% PCE for single crystalline silicon<sup>3</sup>. Despite of that, laborious techniques, extreme pure materials and high manufacturing costs are required to fabricate these devices<sup>4</sup>.

In order to reduce the costs, the second generation of solar cells, based on thin film solar cells were developed. In this group, cadmium telluride (CdTe) and copper indium gallium selenide (CIGS), reaching a maximum efficiency of 23%, are the most remarkable ones<sup>3</sup>. They are cheaper and more flexible, but their efficiencies are lower and the toxicity of these materials suppose a significant problem<sup>4</sup>.

Third generation solar cells arose with the purpose to maintain and improve the efficiency reached by the first generation but also to reduce the costs and toxicity problems of the device fabrication that presented the second generation. These cells are emerging PV technologies and include promising alternatives such as gallium arsenide single junction, Dye-sensitized solar cells, quantum dot cells, perovskites solar cells, etc<sup>4</sup>. Among them, multi-junction solar cells are the most efficient ones up to date, reaching the 44.4% of efficiency for GaAs based multi-junction solar cell<sup>3</sup>.

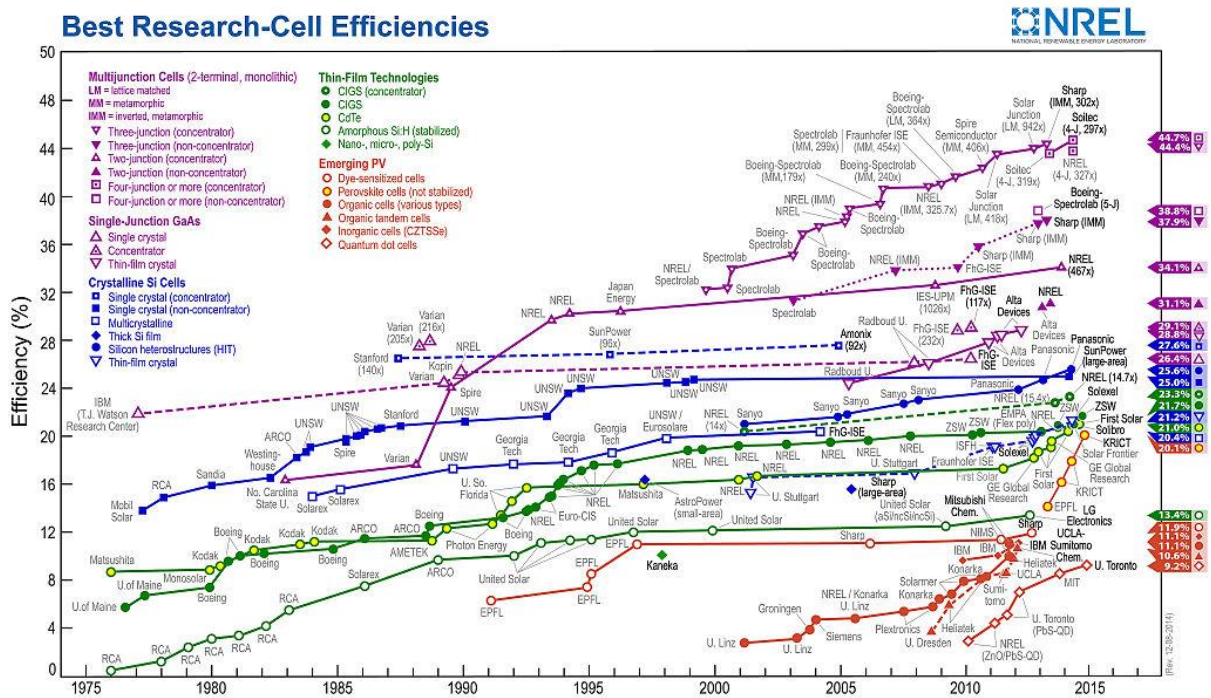


Figure 1: timeline of solar cell energy conversion efficiency since 1976 (NREL Copyright)

Among the emerging PV solar cell technologies, perovskites have become a of a great importance in the fields of material research due to the high efficiency they have shown until the moment, which reached 9.7% in 2012 and 17.9% in 2014.

The investigation and development of this emerging technology is providing day by day new materials, structural modifications and strategies to optimize perovskite cells and make possible the achievement of higher efficiencies<sup>5</sup>.

The present work was done between November and December of 2014 in Institute of Chemical Research of Catalonia (ICIQ), with Dr. Emilio Palomares' Organic Photovoltaic Devices and Application of Quantum Dots Investigation Group.

## Objectives

The main objectives of this work were:

- Synthesize at least 70 mg of a novel molecule for being used as a hole transporting material in perovskite solar cells, and characterize it with  $^1\text{H}$ -RMN,  $^{13}\text{C}$ -RMN and MS.
- Fabricate and characterize various solar cells, some with the novel molecule synthesized and the others with the most used Hole Transporting Material in these devices Spiro-OMeTad, in order to compare them.

# Fundamentals of Perovskites Solar Cells

## 1. Photovoltaic systems

Photovoltaic systems are based on the direct conversion of sunlight into electricity through photovoltaic conversion. This is carried out by devices called solar cells.

A solar cell is basically formed with 3 principal elements: a n-type semiconductor, an pn junction interface and a p-type semiconductor. When sun light impacts to the cell surface, electron-hole pairs are generated and a potential difference between the two semiconductors is created. When the circuit is closed, electrical current is generated.

Since this electrical current is direct and is just produced when the cell is illuminated, solar cells require current accumulation and storage systems, direct to altern current conversion equipments and an electrical grid connection equipment<sup>6</sup>.

## 2. Overview of electrical properties of a semiconductor

In terms of electrical features, materials can be categorised into conductors, insulators or semiconductors, depending on their electrical resistivity, or in another words, their ability to conduct electricity.

A good conductor is a material with an electrical resistivity of more or equal to  $10^{-6} \Omega \text{ cm}$ , while a bad conductor has a resistivity of  $10^6 \Omega \text{ cm}$  or less. Between these two kinds, semiconductors are materials that at 0°K, exhibit a medium electrical resistivity<sup>6</sup>.

Electrical conductivity of a material can be explained as the ability of the electrons to go from the valence band, the highest filled energy level, to the conduction band, the first unfilled energy level, when they are excited. The amount of energy required for that is known as bandgap, and is an inherent property of the material.

Conductor materials such as metals have an excellent electrical conductivity due to overlap between the valence and the conduction bands, so the bandgap is very low. On the contrast, insulators have a bandgap much higher, owing to the distance between bands. Again, a semiconductor is a material that has mixed properties.

When an electron is thermally excited from the valence band to the conduction band in a semiconductor, it leaves behind a vacancy, known as "hole". This hole, understood as a lack of negative charge, can be considered as a particle with positive charge. In order to achieve the

best energetic equilibrium, there will be an intern reorganization of the valence band: the vacancy produced by every electron will be filled by another electron, and thus every hole produced will flow through the net to a minimum energy level. So in general terms, we can think of a dual and opposite conductivity taking place in a semiconductor: electron conductivity and hole flow.

### 3. Perovskites solar cells: main components

The composition of a Perovskites solar cell is very similar to many other 3<sup>rd</sup> generation cells but has the particular of using a halide perovskite as the sensitizer. Basically and as seen in Figure 3, these cells consist in several thin layers of different materials placed between two electrodes, :

#### 3.1 .Working electrode:

The working electrode is a nanocrystalline semiconductor material immobilized onto a conductive substrate, and is responsible for the electron injection and collection and the releasing of them to the circuit.

The most extensively semiconductor material used as a working electrode is mesoporous TiO<sub>2</sub> layer immobilized onto FTO glass substrate, although other n-type semiconductors has been tested<sup>4</sup>.

In order to avoid that the HTM could penetrate the FTO, another layer is needed between mp-TiO<sub>2</sub> and the FTO glass. This blocking layer is a compact layer of TiO<sub>2</sub> placed between the mp-TiO<sub>2</sub> and the FTO. If this blocking layer was not present and the HTM could contact with the FTO, a recombination would happen, leading to a short circuit and a loss of current<sup>4</sup>.

#### 3. 2. Perovskite semiconductor

This layer has a fundamental role in a solar cell, because it acts as the absorber of sunlight and is where electron-hole pairs are generated. In perovskites cells, organic-inorganic halides with perovskite ABX<sub>3</sub> crystal structure materials are used as visible-light sensitizers, such as CH<sub>3</sub>NH<sub>3</sub>PbBr<sub>3</sub> or CH<sub>3</sub>NH<sub>3</sub>PbI. These materials can be synthesized from different substances, and because of the optic and electric properties they present and their ability to generate excitons (electron-hole pairs), they are a very promising for solar cells<sup>7</sup>.

Figure 2 shows the crystall structure for perovskite compounds

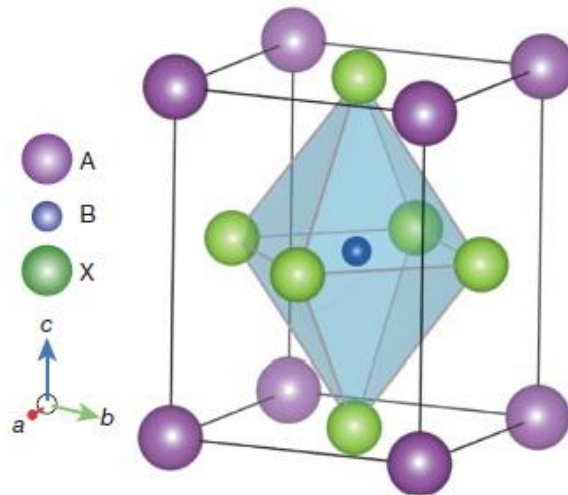


**Figure 2:** Unit cell of the most commonly employed perovskite absorber in solar cells, where A is methylammonium, B is Pb and X is I or Cl (adapted from<sup>8</sup>).

### 3.3. Hole Transporting Material (HTM)

The HTM has the role to collect the holes produced in the perovskite layer and transfer them to the counter electrode. It is mainly an organic material, though there are also interesting inorganic HTM.

The ideal HTM must have two essential characteristics<sup>4</sup>:

- The HOMO (Highest Occupied Molecular Orbital) of the HTM has to be of a higher energy than the LUMO (Lowest Unoccupied Molecular Orbital) of the perovskite material, so that the holes can jump from the perovskite to the HTM.
- HTM should have a good solubility into the mp-TiO<sub>2</sub> layer, so it can fill homogeneously every porous of it, but it must not go through the blocking layer.

Other interesting characteristics would be that they were highly transparent so they do not interfere in the perovskite absorbance and that they have to be easy and cheap to prepare.

One of the best and most efficient HTM nowadays is the organic material 2,2',7,7'-tetrakis(N,N-di-p-methoxyphenylamine)9,9'-spirofluorene, known commonly as Spiro-OMeTAD, which has reached the efficiency of 15.4% with perovskite solar cells<sup>8</sup>. However, it is highly expensive due to its multistep synthesis; so many other alternatives as HTM are being investigated.

### 3.4. Counter electrode

The counter electrode consist material with high conductivity and mechanical and chemical stability. It is usually a layer made of a noble metal, such as gold, platinum or silver<sup>4</sup>.

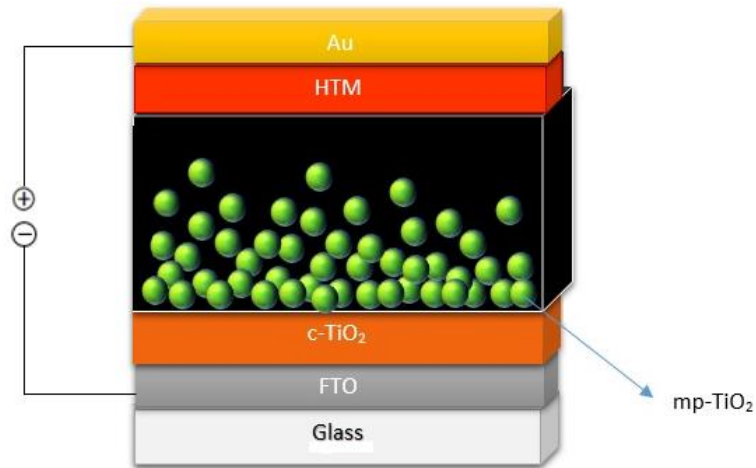


**Figure 3:** scheme of the different layers of a perovskite solar cell

#### 4. Operation of perovskites solar cells

The incoming light is absorbed by the perovskite material and an electron-hole pair is created. The electron created is excited to the highest occupied molecular orbital (HOMO) to the lowest unoccupied molecular orbital (LUMO) of the perovskite. Then, the electron is split from the perovskite LUMO to the mp-TiO<sub>2</sub> conduction band. After that, the electron travels by diffusion through the d-TiO<sub>2</sub> and is collected at the substrate contact (FTO glass), to be finally released to the external circuit.

On the other hand, the hole generated flows from the HOMO to the lower energy levels of the perovskite, to be finally transferred to the HTM. There the hole is transported via hopping to the counter electrode to be released to the external circuit<sup>4</sup>.

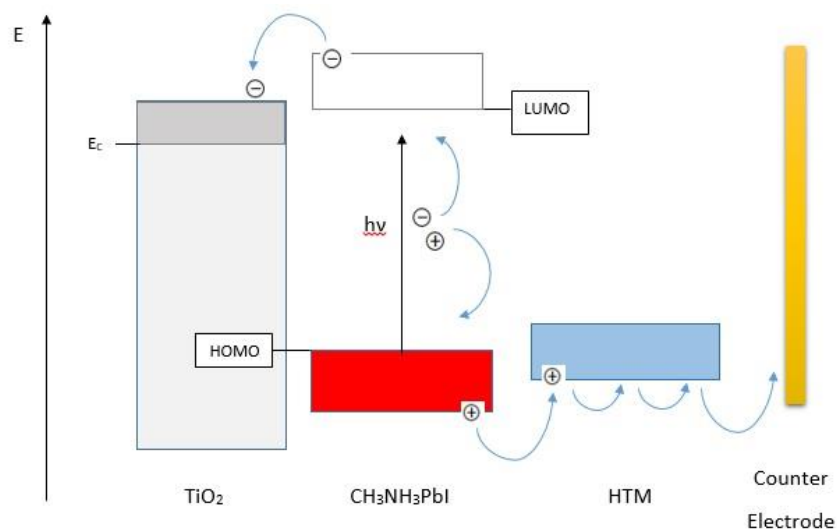


**Figure 4:** Energy levels of the TiO<sub>2</sub>/CH<sub>3</sub>NH<sub>3</sub>PbI/HTM junction, showing that the HOMO and the LUMO of CH<sub>3</sub>NH<sub>3</sub>PbI are well positioned for electron injection into TiO<sub>2</sub> and hole transfer to the HTM.

## 5. Solar cells characterization

Solar cells are characterized through the current and the voltage measures, and the curves represented with these data. From these data obtained we can calculate the fill factor, the maximum power and the power efficiency conversion, which is the overall efficiency of the solar cell to convert the incident light into electric energy.

Given a typical graphic I-V we can see the represented curve passes through two significant points the  $V_{oc}$  and the  $J_{sc}$ :

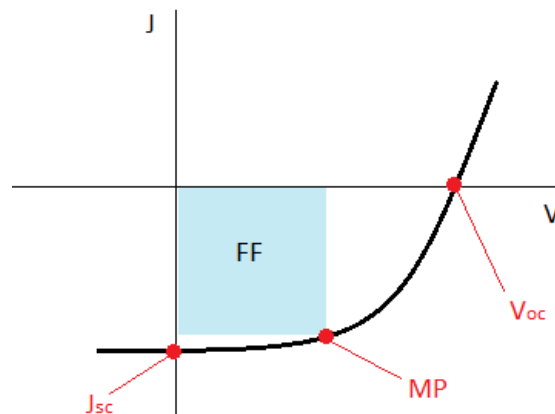


**Figure 5:** Typical I-V curve, where the parameters to determine the efficiency of the cell are marked:  $V_{oc}$ ,  $J_{sc}$ , MP and FF

The open circuit voltage ( $V_{oc}$ ) is the point found when the current is zero and represents the difference of electrical potential between the two terminals of the solar cell when the circuit is open, disconnected from the current.  $V_{oc}$  depends mainly on the energetic level of the semiconductor frontier orbitals, but can be influenced by charge recombination processes<sup>9</sup>.

The short circuit current ( $J_{sc}$ ) is the point found when the voltage is zero and represents the maximum current that can be obtained in a solar cell. The  $J_{sc}$  depends on many parameters, such as the thickness of the solar cell or the ability of the device to harvest more photons within the solar spectrum, but mainly on the number of absorbed photons that can be converted to energy<sup>9</sup>. It also depends on the area of the photoactive layer, so it is obtained with the current when the voltage is zero divided by the area of the cell:

$$J_i = \frac{I_{iv=0}}{A} \quad (1)$$

The power of the cell is defined as the product of the voltage times current. The maximum power (MP) represents the maximum efficiency of the solar device in converting sunlight into electricity<sup>10</sup> and it is obtained via (2):

$$MP = / V \times I / \max_{(0 \leq V \leq V_{oc})} \quad (2)$$

The fill factor (FF) is a percentage that describes how ideal is the curve I-V obtained, and gives an idea of the degree to which the voltage at the maximum power point ( $V_{ff}$ ) matches the  $V_{oc}$  and that the current at the maximum power point ( $J_{ff}$ ) matches the  $J_{sc}$ . Ideally, the values for the  $J_{ff}$  and  $V_{ff}$  have to coincide the most possible with  $J_{sc}$  and  $V_{oc}$ . When that happens, FF has a value close to 100 and the power efficiency of the cell is high<sup>9, 10</sup>.

Graphically, the FF is also the area of the largest rectangle which will fit in the IV curve. So ideally, the obtained curve must be as squared as possible.

FF can be calculated with  $V_{oc}$ ,  $J_{sc}$  and MP values using the expression (3):

$$FF (\%) = \frac{MP}{V_{oc} \times J_{sc}} \times 100 \quad (3)$$

Power conversion efficiency (PCE or  $\eta$ ) is a parameter defined as the ratio of the sun energy incident on the cell and the electrical energy finally generated. This is the most commonly used parameter to compare the performance of one solar cell to another<sup>10</sup>.

PCE is determined by the photocurrent density at short circuit ( $J_{sc}$ ), the open circuit voltage ( $V_{oc}$ ), the fill factor (FF) obtained and the power of the incident light ( $P_{light}$ ), using the following expression<sup>10</sup>:

$$PCE = \frac{J_{sc} \times V_{oc} \times FF}{P_{light}} \quad (4)$$

As the PCE strongly depends on the intensity of the incident sunlight ( $P_{light}$ ) and the temperature of the cell, conditions under which the current and the voltage are measured must be carefully controlled. Nowadays, standard tests conditions for solar cells are generally AM 1.5 sunlight spectrum, at an irradiance ( $P_{light}$ ) of 100 mW/cm<sup>2</sup> and a temperature of 25°C<sup>9</sup>.

To get to that conditions, various standard test conditions have been defined. Figure 6 shows the different paths lengths considered to achieve the conditions:

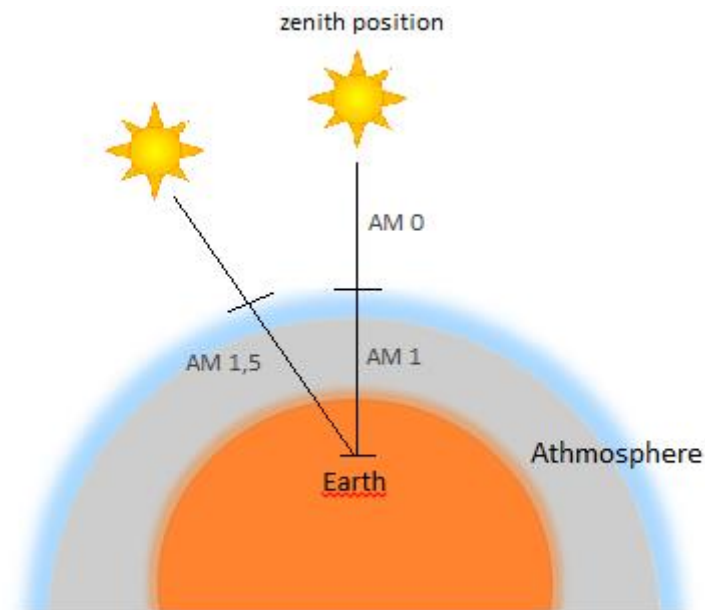


**Figure 6:** Schematic representation of the path length and its dependence on the zenith angle.

Solar radiation intensity is defined in terms of air mass (AM), which represents the reduction in the power of light when it passes through the atmosphere before striking the Earth surface, due to air, dust, particles, etc. As a reference, it is considered that in space the solar light has an AM of 0, whatever the sun position may be, and the light AM when it strikes the Earth surface is 1 when the sun is at zenith position. Given that the sun is located at zenith for a short period of time, the standard value of AM for measurements is 1.5. In another words, 1.5 is the the atmosphere length considered that the light must go through to arrive to Earth Surface, referring when the sun is at zenith<sup>9</sup>.

The PCE of a solar cell is influenced by many things that make impossible that all the incident energy in a solar cell can be converted into electrical energy<sup>9</sup>:

- Recombination process: recombination processes are phenomena that can occur while the pair electron-hole are generated and separated, and consist in the reunion of both before they can join the electrical circuit and contribute to the current of the cell. When this recombination occurs, the  $V_{oc}$  gets lower, and thus the efficiency.
- Temperature: rising the operating temperature of a solar cell increases the recombination process, so they work best at low temperatures. Commonly solar cells are measured at 25 °C.
- Resistance: the electrical resistivity of the cell material itself reduce the conductivity ability and in overall the cell efficiency

- Light Harvesting Efficiency (LHE): capacity of the cell to absorb the photons from the incident light. It is determined by the molar extinction coefficient and the concentration of the absorber molecule and the optical path length, according to Lambert-Beer's law. In consequence, it is a property of the material.
- Reflection: natural loss of light when it is reflected away from the cell's surface and not harvested.
- Bandgap energy: it is needed a minimum amount of energy to generate a pair electron-hole and it depends on the material itself. In principle, photons with energy lower than the bandgap energy of the absorber layer are not absorbed and do not generate electron-hole pairs. These photons represents one of the main losses in the energy conversion process in solar cells.

## 6. Synthesis of a novel indoline derivative HTM

Indoline derivative compounds have properties that make them good candidates for playing the role of HTM in solar cells. To date, they have been commonly used as sensitizers due to its high light-harvesting efficiency, but the good pore filling into the mp-TiO<sub>2</sub> layer and the high V<sub>oc</sub> that devices with indoline derivatives present, can make them suitable to operate as the HTM<sup>11</sup>.

Not only have they the essential characteristics in a HTM, but most of them have an easy and a cheap synthesis and purification<sup>11</sup>.

Here, the synthesis of the proposed novel indoline derivative, **ML01**, is relative short synthesis of 5 step-process. The presence of O<sub>2</sub> or humidity is a problem in these kind of synthesis, because of the use of some reagents that could react in contact with air, like n-BuLi, or that are sensitive to air, like Pd(PPh<sub>3</sub>)<sub>4</sub>. Thus, in order to avoid that and maintain the purity of the products, the whole synthesis was performed in a schlenk system.

## Experimental Section

### 1. Table of reactives

The following table shows the characteristics of purity, toxicity and manipulation of the substances used in the experimental section, according to Regulation (EC) No. 1272/2008<sup>12</sup>.

**Table 1:** Reactives used in Experimental Section, with their purity, toxicity characteristics and equipment required for its safe manipulation indicated.

Substance	Purity (%)	Toxicity	Manipulation
Acetic acid	99.0	<ul style="list-style-type: none"> <li>- Acute toxicity: Oral (4)</li> <li>- Skin irritation (2)</li> <li>- Eye irritation (2)</li> <li>- Specific target organ toxicity – single exposure - : respiratory system (3)</li> <li>- Aquatic acute (1)</li> <li>- Aquatic chronic (1)</li> </ul>	<ul style="list-style-type: none"> <li>- Glasses</li> <li>- Gloves</li> <li>- Lab coat</li> <li>- Fume cabinet</li> <li>- Handle away from ignition sources</li> </ul>
Acetonitrile	99.8	<ul style="list-style-type: none"> <li>- Acute toxicity:</li> <li style="padding-left: 20px;">Oral (4)</li> <li style="padding-left: 20px;">Vapour (4)</li> <li style="padding-left: 20px;">Dermal (4)</li> <li>- Eye irritation (2)</li> </ul>	<ul style="list-style-type: none"> <li>- Glasses</li> <li>- Gloves</li> <li>- Lab coat</li> <li>- Fume cabinet</li> <li>- Handle away from ignition sources</li> </ul>
Acetone	99.8	<ul style="list-style-type: none"> <li>- Eye irritation (2)</li> <li>- Specific target organ toxicity – single exposure – (3)</li> </ul>	<ul style="list-style-type: none"> <li>- Glasses</li> <li>- Gloves</li> <li>- Fume cabinet</li> <li>- Lab coat</li> <li>- Handle away from ignition sources</li> <li>- Handle in ventilate places</li> </ul>
Bis(trifluoromethane)-sulfonimide lithium salt	99.9	<ul style="list-style-type: none"> <li>- Skin corrosion(1B)</li> <li>- Acute toxicity:</li> </ul>	<ul style="list-style-type: none"> <li>- Glasses</li> <li>- Gloves</li> </ul>

		<p>Oral (3)</p> <p>Dermal (3)</p> <p>- Specific target organ toxicity – repeated exposure – (2)</p> <p>- Chronic aquatic toxicity (3)</p>	<p>- Fume cabinet</p> <p>- Lab coat</p>
Chlorobenzene	≥99.5	<p>- Flammable liquids (3)</p> <p>- Skin irritation (2)</p> <p>- Chronic aquatic toxicity (2)</p> <p>- Acute toxicity:</p> <p>Oral (4)</p> <p>Inhalation (4)</p>	<p>- Glasses</p> <p>- Gloves</p> <p>- Fume cabinet</p> <p>- Lab coat</p> <p>- Handle away from ignition sources</p>
Chloroform	≥99.5	<p>- Acute toxicity :</p> <p>Oral (4)</p> <p>Inhalation (3)</p> <p>- Skin irritation (2)</p> <p>- Eye irritation (2)</p> <p>- Carcinogenicity(2)</p> <p>- Specific target organ toxicity – single exposure – : central nervous system (3)</p> <p>- Specific target organ toxicity – repeated exposure – (1)</p>	<p>- Glasses</p> <p>- Gloves</p> <p>- Fume cabinet</p> <p>- Lab coat</p>
Copper	99.9	<p>- Acute aquatic toxicity (1)</p> <p>- Chronic aquatic toxicity (3)</p>	<p>- Handle away from ignition sources</p> <p>- Handle in ventilate places</p>
4,7-dibromobenzo[c]-1,2,5-thiadiazole	95.0	<p>- Acute toxicity: Oral (3)</p>	<p>- Glasses</p> <p>- Gloves</p> <p>- Lab coat</p> <p>- Handle in ventilate places</p>

1,2-dichlorbenzene	99.0	<ul style="list-style-type: none"> <li>- Acute toxicity: Oral (4)</li> <li>- Skin irritation (2)</li> <li>- Eye irritation (2)</li> <li>- Specific target organ toxicity – single exposure - : respiratory system (3)</li> <li>- Acute aquatic toxicity (1)</li> <li>- Chronic aquatic toxicity (1)</li> </ul>	<ul style="list-style-type: none"> <li>- Glasses</li> <li>- Gloves</li> <li>- Lab coat</li> <li>- Fume cabinet</li> <li>- Handle away from ignition sources</li> </ul>
Dichloromethane	≥99.5	<ul style="list-style-type: none"> <li>- Skin irritation (2)</li> <li>- Eye irritation (2)</li> <li>- Carcinogenicity(2)</li> <li>- Specific target organ toxicity – single exposure - : respiratory system, central nervous system (3)</li> <li>- Specific target organ toxicity – repeated exposure – (2)</li> </ul>	<ul style="list-style-type: none"> <li>- Glasses</li> <li>- Gloves</li> <li>- Lab coat</li> <li>- Fume cabinet</li> </ul>
1,2,3,4-tetrahydro-cyclop[ <i>b</i> ]indole	96.0	<ul style="list-style-type: none"> <li>- Skin irritation (2)</li> <li>- Eye irritation (2)</li> <li>- Specific target organ toxicity –single exposure – (3)</li> </ul>	<ul style="list-style-type: none"> <li>- Glasses</li> <li>- Gloves</li> <li>- Fume cabinet</li> <li>- Lab coat</li> </ul>
Ethanol	≥99.8	<ul style="list-style-type: none"> <li>- Flammable liquid (2)</li> </ul>	<ul style="list-style-type: none"> <li>- Glasses</li> <li>- Gloves</li> <li>- Lab coat</li> <li>- Fume cabinet</li> <li>- Handle away from ignition sources</li> </ul>
Ethyl Acetate	99.8	<ul style="list-style-type: none"> <li>- Flammable liquid (2)</li> <li>- Eye irritation (2)</li> <li>- Specific target organ toxicity –single exposure – : central nervous system (3)</li> </ul>	<ul style="list-style-type: none"> <li>- Glasses</li> <li>- Gloves</li> <li>- Lab coat</li> <li>- Fume cabinet</li> </ul>

			- Handle away from ignition sources
Gold	99.9	Not a hazardous substance	- Handle in ventilate places
Hexane	95.0	<ul style="list-style-type: none"> <li>- Skin irritation (2)</li> <li>- Reproductive toxicity (2)</li> <li>- Specific target organ toxicity – single exposure – : central nervous system (3)</li> <li>- Specific target organ toxicity – repeated exposure – (2)</li> <li>- Aspiration hazard (1)</li> <li>- Chronic aquatic toxicity (2)</li> </ul>	<ul style="list-style-type: none"> <li>- Glasses</li> <li>- Gloves</li> <li>- Fume cabinet</li> <li>- Lab coat</li> <li>- Handle away from ignition sources</li> </ul>
4-iodotoluene	99.0	Not a hazardous substance	- Handle in ventilate places
2-Isopropoxy-4,4,5,5-tetramethyl-1,3,2-dioxaborolane	98.0	<ul style="list-style-type: none"> <li>- Skin irritation (2)</li> <li>- Eye irritation (2)</li> <li>- Specific target organ toxicity – single exposure – (3)</li> </ul>	<ul style="list-style-type: none"> <li>- Glasses</li> <li>- Gloves</li> <li>- Fume cabinet</li> <li>- Lab coat</li> <li>- Handle away from ignition sources</li> </ul>
Lead(II) chloride	98.0	<ul style="list-style-type: none"> <li>- Reproductive toxicity (1)</li> <li>- Acute toxicity:</li> <li>- Acute toxicity:</li> <li>Inhalation (4)</li> <li>Oral (4)</li> <li>- Specific target organ toxicity – repeated exposure – (2)</li> <li>- Acute and chronic toxicity (1)</li> </ul>	<ul style="list-style-type: none"> <li>- Glasses</li> <li>- Gloves</li> <li>- Lab coat</li> <li>- Avoid long exposure</li> </ul>
Methanamine hydriodide	98	<ul style="list-style-type: none"> <li>- Acute toxicity: Oral (4)</li> <li>- Skin irritation (2)</li> <li>- Eye irritation (2)</li> </ul>	<ul style="list-style-type: none"> <li>- Glasses</li> <li>- Gloves</li> <li>- Fume cabinet</li> </ul>

		- Specific target organ toxicity – single exposure – : respiratory system (3)	- Lab coat - Handle in ventilate places
N-bromosuccinimide	99.0	- Acute toxicity: Oral (4) - Skin corrosion(1)	- Glasses - Gloves - Lab coat - Handle in ventilate places
n-Butyllithium solution		- Highly - Flammable liquid and vapour - Catches fire spontaneously if exposed to air - Violently reaction with water - Acute toxicity - Skin irritation (2) - Eye irritation (2) - Harmful to health by prolonged exposure through inhalation - Toxic to aquatic organisms	- Glasses - Gloves - Mask - Fume cabinet - Lab coat - Handle away any ignition sources - Handle under inert gas; avoid contact with air - Avoid direct contact with water
<i>N,N</i> -Dimethyl-formamide	≥99.8	- Eye irritation (2) - Reproductive toxicity (1B) - Flammable liquid (3) - Acute toxicity: Inhalation (4) Dermal (4)	- Glasses - Gloves - Lab coat - Fume cabinet - Avoid long exposure - Handle away from ignition sources
Potassium carbonate	≥99.0	- Acute toxicity: Oral (4) - Skin irritation (2) - Eye irritation (2) - Specific target organ toxicity– single exposure – : respiratory system (3)	- Glasses - Gloves - Fume cabinet - Lab coat

			- Handle in ventilate places
Sodium borohydride	≥99.0	- Emit flammable gases in contact with water - Acute toxicity: Dermal (3) Oral (3) - Skin corrosion(1)	- Glasses - Gloves - Fume cabinet - Lab coat - Handle in ventilate places
Sodium sulfate anhydrous	≥99.0	Not a hazardous substance	- Handle in ventilate places
Spiro-MeOTAD	99.0	Not a hazardous substance	- Handle in ventilate places
4- <i>tert</i> -Butylpyridine	96.0	- Skin irritation (2) - Eye irritation (2) - Specific target organ toxicity – single exposure – : respiratory system (3)	
Tetrahydrofuran	≥99.9	- Flammable liquid (2) - Eye irritation (2) - Carcinogenicity(2) - Specific target organ toxicity – single exposure – : respiratory system (3)	- Glasses - Gloves - Lab coat - Fume cabinet - Handle away from ignition sources
Tetrakis(triphenylphosphine)palladium(0)	99.0	Not a hazardous substance	- Handle in ventilate places
Titania paste (18 NR-T dyesol)		- Skin irritation (2) - Eye irritation (2) - Specific target organ toxicity – single exposure – : respiratory system (3)	- Glasses - Gloves - Lab coat - Fume cabinet - Handle away from ignition sources

Titanium(IV) chloride	99.0	<ul style="list-style-type: none"> <li>- Acute toxicity:</li> <li>  Vapour (2)</li> <li>- Skin corrosion(1)</li> <li>- Specific target organ toxicity– single exposure – (1)</li> <li>- Specific target organ toxicity– repeated exposure – (1)</li> </ul>	<ul style="list-style-type: none"> <li>- Glasses</li> <li>- Gloves</li> <li>- Fume cabinet</li> <li>- Lab coat</li> </ul>
Titanium diisopropoxide bis(acetylacetonate) solution (75 wt.% in isopropanol)		<ul style="list-style-type: none"> <li>- Flammable liquid (2)</li> <li>- Skin irritation (2)</li> <li>- Eye irritation (2)</li> <li>- Specific target organ toxicity– single exposure – : respiratory and central nervous system (3)</li> </ul>	<ul style="list-style-type: none"> <li>- Glasses</li> <li>- Gloves</li> <li>- Lab coat</li> <li>- Fume cabinet</li> <li>- Handle away from ignition sources</li> </ul>
Zinc	≥98.0	<ul style="list-style-type: none"> <li>- Acute aquatic toxicity (1)</li> <li>- Chronic aquatic toxicity (1)</li> </ul>	<ul style="list-style-type: none"> <li>- Handle in ventilate places</li> </ul>

## 2. Synthesis of ML01

The synthesis of **ML01** is a 5 step-process starting from a commercial indole and including an Ullman reaction (i), a reduction (ii), a bromination (iii), a substitution Br-B (iv) and a Suzuki reaction (v) as seen in Figure 7:

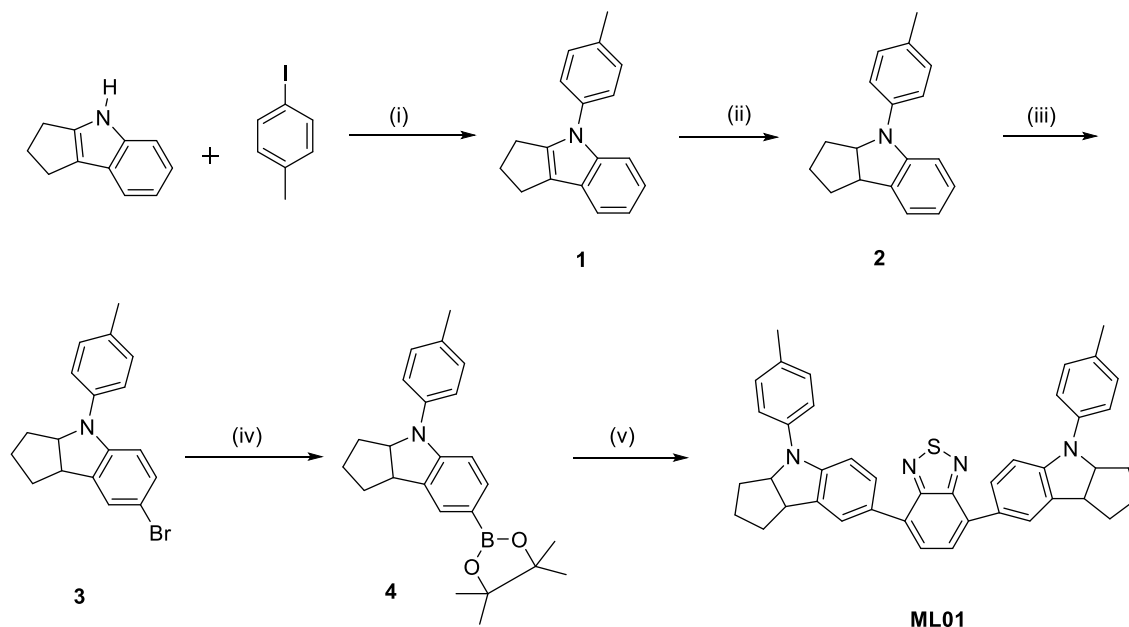


**Figure 7:** Global scheme for the synthesis of **ML01** via a 5-step reaction

### 2.1. Synthesis of 4-(p-tolyl)-1,2,3,4-tetrahydrocyclopenta[b]indole (1):

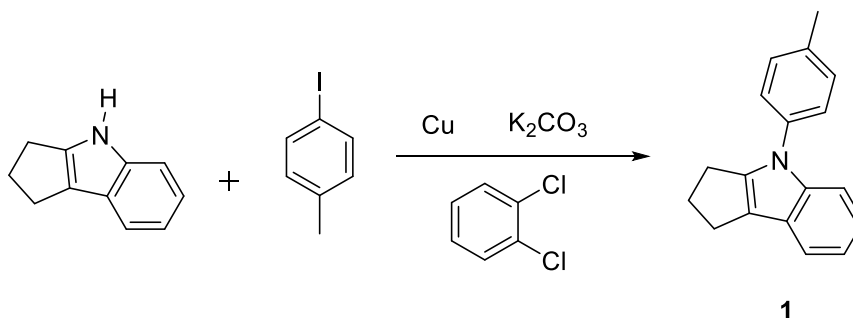


**Figure 8:** Scheme of step 1 of the synthesis of **ML01**

The reaction consists in a nucleophilic substitution between an aryl iodide, acting as the electrophile, and an amine, acting as the nucleophile.

In a 250 ml flask a mixture of 3,4-dihydrocyclopenta[b]indole (1.9g, 12.08mmol), 1-iodo-4-methylbenzene (3g, 14mmol), copper (0.122g, 1.92mmol) and potassium carbonate (3.48g, 25.2mmol) was added. Then, 60 ml of 1,2-dichlorobenzene were added, and the solution was

heated up to 150°C during 48 hours. At first the solution was brownish-red and gradually became darker.

After 48 hours, a TLC was performed, using Hexane/Ethyl Acetate (9.5:0.5), to verify if any product has been formed. Since that was the case, the solvent was distilled and the remaining mixture was extracted with CH<sub>2</sub>Cl<sub>2</sub>. The extracted layer was dried over Na<sub>2</sub>SO<sub>4</sub> anhydrous, and then concentrated with a under reduced pressure. After that, the yellowish crude was purified by column chromatography on silica gel, eluting with Hexane/Ethyl Acetate (9.5:0.5), to obtain a yellow oil.

## 2. 2. Synthesis of 4-(p-tolyl)-1,2,3,3a,4,8b-hexahydrocyclopenta[b]indole (2):

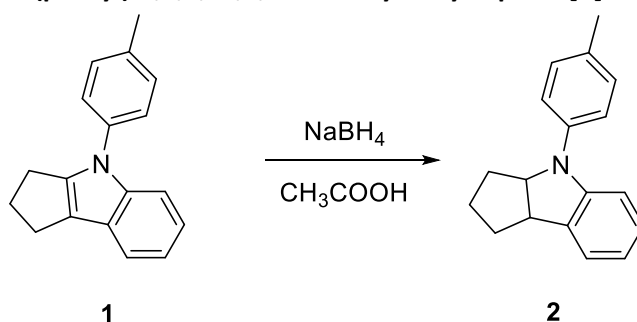


**Figure 9:** Scheme of step 2 of the synthesis of **ML01**

Once the obtention of the product 1 had been verified with <sup>1</sup>H-RMN step two can be started. This step is a reduction of the double bond using sodium borohydride.

In a 50 ml flask the yellow oil from 1 (0.15g, 0.42mmol) and acetic acid (4ml) were added. Slowly NaBH<sub>4</sub> was then added (0.22g, 5.86mmol) and while was added the mixture started to bubble.

The mixture was then heated up to 70°C and stirred during 12 hours. Eventually the mixture went from light yellow to blue.

After that time, product formation was verified by TLC, using Hexane/CH<sub>2</sub>Cl<sub>2</sub> (9.5:0.5) as the eluent.

After that, a Na<sub>2</sub>CO<sub>3</sub> saturated solution was added to the mixture in order to increase the pH until 7. While the pH was growing, the solution colour changed from blue to green. Then the resulting mixture was extracted with CH<sub>2</sub>Cl<sub>2</sub> and the extracted layer was dried over Na<sub>2</sub>SO<sub>4</sub> anhydrous.

Finally the crude was concentrated and purified by column chromatography on silica gel, using Hexane/CH<sub>2</sub>Cl<sub>2</sub> (9.5:0.5) as the eluent, to obtain the product as a yellow oil.

### 2. 3. Synthesis of 7-bromo-4-(p-tolyl)-1,2,3,3a,4,8b-hexahydrocyclopenta[b]indol (3):

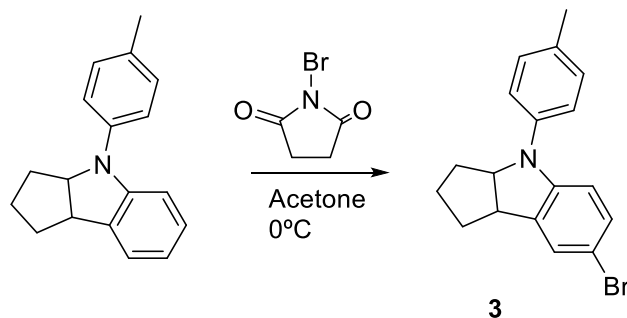


**Figure 10:** Scheme of step 3 of the synthesis of **ML01**

After verifying that the product 2 was successfully formatted with  $^1\text{H-RMN}$ , we can proceed with the synthesis. The next step consists in a bromination of the aril using N-bromosuccinimide. Since this reactive is sensitive to light, the reaction had to be performed in the dark.

In a 100 ml schlenk flask a solution of 4-(p-tolyl)-1,2,3,3a,4,8b-hexahydrocyclopenta[b]indole (0.461g, 1.85mmol) and acetone (20 ml) were added.

The flask was adapted into an ice-water bath in order to cool the mixture to 0°C.

Once cooled, NBS (0.329g, 1.85mmol) was added and the mixture was stirred in the dark for 2 hours. After that time, a TLC was performed in order to check if any product had been formed, eluting with Hexane. Since that was the case, the resulting crude product, which had a vibrant blue colour, was extracted with  $\text{CHCl}_3$  and the organic layer was dried over  $\text{Na}_2\text{SO}_4$ . The resulting mixture was concentrated and recrystallized in Hexane to obtain a white solid.

### 2. 4. Synthesis of 7-(4,4,5,5-tetramethyl-1,3,2-dioxaborolan-2-yl)-4-(p-tolyl)-1,2,3,3a,4,8b-hexahydrocyclopenta[b]indole (4):

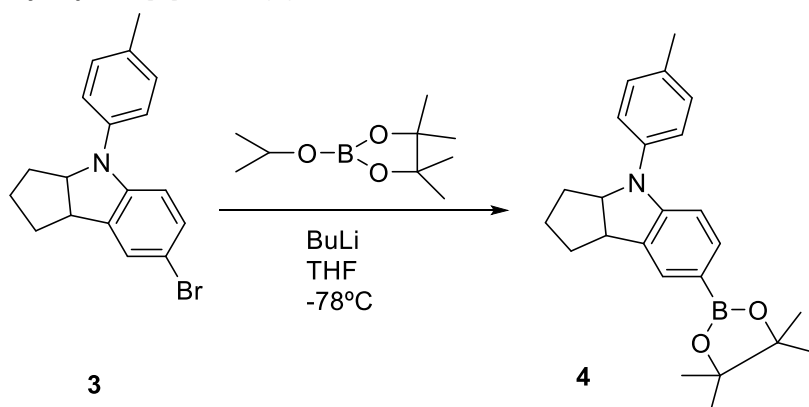


**Figure 11:** Scheme of step 4 of the synthesis of **ML01**

Since the product **3** had been verified with <sup>1</sup>H-RMN, step 4 could be begun. As our target molecule is synthesized by a Suzuki reaction, the precursors had to be prepared, so previously to the Suzuki reaction the desired indoline boronate had to be prepared.

In a 100 ml schlenk flask, compound **3** (0.100g, 0.305mmol) was dissolved in dry THF (10 ml). The flask was then adapted into an acetone-dry CO<sub>2</sub> bath in order to cool the solution to -78°C.

Once the solution was cooled, very carefully, BuLi (0.150ml, 0.366mmol) was added using a syringe previously purged. After an hour, pinacol borate (0.075 ml, 0.366mmol) was added. Then, the mixture was stirred for 6 hours.

After that, a TLC was performed to verify if the reaction was successful, using Hexane/ethyl acetate (9.5:0.5) as the eluent. Since that was the case, the crude mixture was extracted with ethyl acetate and the extracted layer was dried over Na<sub>2</sub>SO<sub>4</sub> anhydrous. The resulting dark green solution was concentrated and purified by column chromatography, eluting first with Hexane/CH<sub>2</sub>Cl<sub>2</sub> (9.5:0.5) and with a major polarity, to obtain a yellow oil.

### 2. 5. Synthesis of ML01:

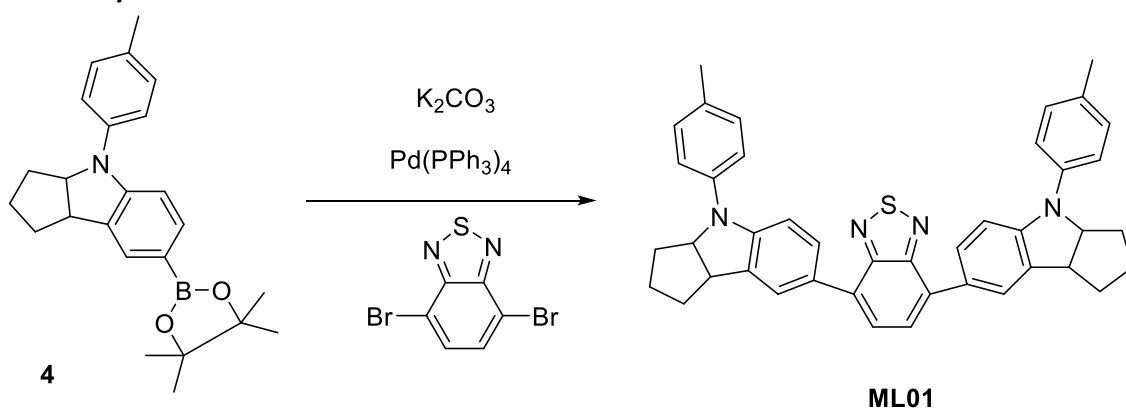


**Figure 12:** Scheme of the final step of the synthesis of **ML01**

The final step is the Suzuki reaction using the indoline boronate precursor synthesized in the previous step.

In a 100 ml Schlenk flask, a mixture of the obtained product **4** (0.068g, 0.181mmol), Pd<sup>0</sup>(PPh<sub>3</sub>)<sub>4</sub> (18.55mg, 0.016mmol) and 4,7-dibromobenzoc[1,2,5]thiadiazole (27.00mg, 0.0907mmol) was added and dissolved in dry THF (10 ml). The flask was then adapted into a N<sub>2</sub> liquid container in order to freeze the mixture, while N<sub>2</sub> gas was injected to the flask. Once it was frozen, the schlenk was submitted into vacuum for 10 minutes in order to degasify the solution. After that time, the flask was removed from the N<sub>2</sub> bath and the solution was stirred until room temperature was reached.

Then, potassium carbonate (0.9 ml, 0.9mmol) was added and the reaction mixture, which had a saturated orange colour, was stirred at 70°C overnight.

Then, a red solution was obtained. It was cooled to room temperature and then a TLC was performed using Hexane/CH<sub>2</sub>Cl<sub>2</sub> as the eluent. Since a product was obtained, the mixture was extracted with CH<sub>2</sub>Cl<sub>2</sub> and the organic layer was dried over Na<sub>2</sub>SO<sub>4</sub>. Then the solution was concentrated, and the resulting red crude product was purified by column chromatography on silica gel, eluting with Hexane/CH<sub>2</sub>Cl<sub>2</sub> (8:2). A red product was finally obtained.

Unfortunately, the <sup>1</sup>H-RMN obtained told us the target molecule was not formed and that just one bromine from the 4,7-dibromobenzo[*c*]-1,2,5-thiadiazole was linked to our indoline boronate, so the reaction performed was:

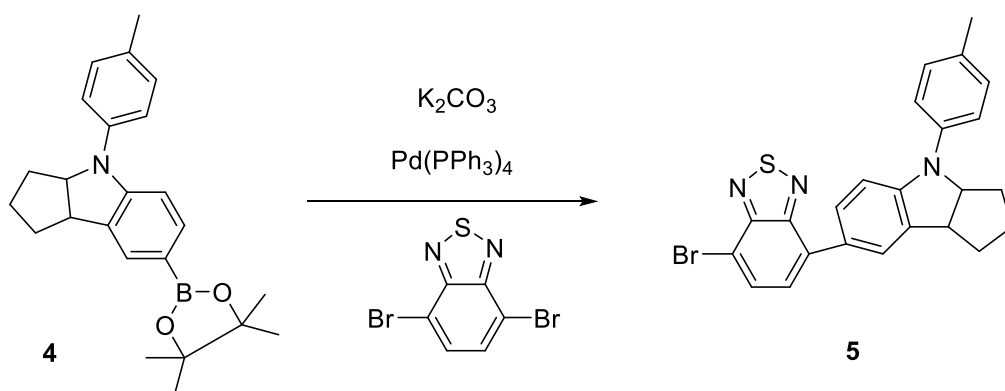


**Figure 13:** Scheme of the real reaction performed the first time step 5 was tried.

Since not all the product **3** was reacted and 0.04g were saved, the reactions iv and v could be repeated and the Suzuki reaction was performed in situ this time. But, given that the product obtained (**5**) can be used instead of 4,7-dibromobenzo[*c*]-1,2,5-thiadiazole and that was already purified, it was used in the next reaction.

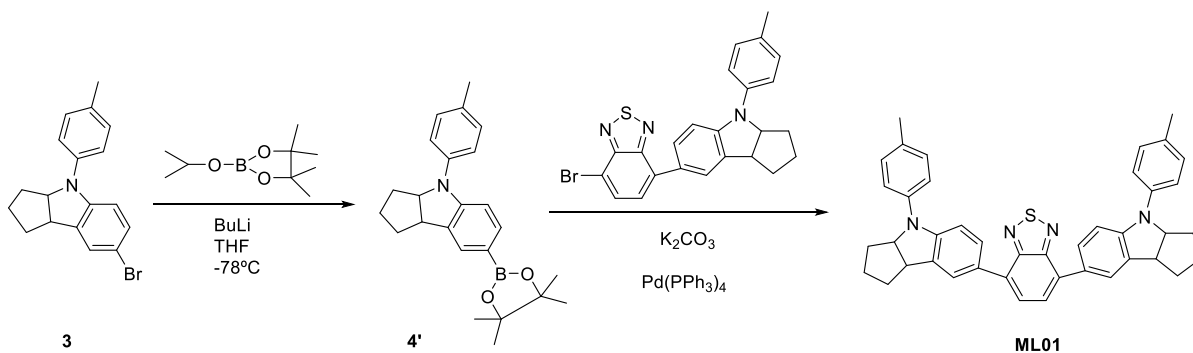


**Figure 14:** Scheme the repetition of the two last steps for the synthesis, performing the Suzuki reaction in situ.

In a 100 ml schlenk flask, compound 3 (0.032g, 0.098mmol) was dissolved in dry THF (10 ml). The flask was then adapted into an acetone-dry CO<sub>2</sub> bath in order to cool the solution to -78°C. Once cooled, BuLi (0.05ml, 0.117mmol) was added carefully. After 1 hour pinacol borate (0.02 ml, 0.117mmol) was added to the solution using a syringe previously purged. The mixture was stirred for 6 hours.

After that, a TLC was performed, using Hexane/CH<sub>2</sub>Cl<sub>2</sub> (9:1) as the eluent, to verify if any product had been formed. Since that was the case and that Suzuki reaction was performed in situ, the product obtained was not purified.

Then, in a 100 ml schlenk flask, Pd(PPh<sub>3</sub>)<sub>4</sub> (10.14mg, 8.78·10<sup>-3</sup>mmol) and compound 5 (54.10mg, 0.117mmol) and THF (10 ml) were added and dissolved. Using a metal cannula, the recently synthesized product 4' was injected to the flask. The reaction mixture was stirred 7 hours at 70°C.

After that time, a TLC was again performed, eluting with Hexane/CH<sub>2</sub>Cl<sub>2</sub> (7:3). The same result as the first time the Suzuki was performed was obtained. Any case, the crude mixture was extracted with CH<sub>2</sub>Cl<sub>2</sub> and the organic layer was dried over Na<sub>2</sub>SO<sub>4</sub>. Then the solution was concentrated, and the resulting red product was purified by column chromatography on silica gel, eluting with Hexane/CH<sub>2</sub>Cl<sub>2</sub> (8:2).

This time, two different products were eluted from the column chromatograph, the first one was red and the second one was pink.

### 3. Device Fabrication

The device fabrication consist in preparing the commercial support of fluorine doped Tin Oxide (FTO) glass and adding progressively the different layers needed to get our perovskite solar cells.

The starting material comes as films of 10 cm with glass and a conductive layer of fluorine doped tin oxide for one side of the film. First of all, FTO glass had to be etched in order to remove the FTO from the extremes parts of the layer. For this purpose, the whole films were covered with adhesive tape. The film must be covered by the FTO side. To know which part is the conductive one we can use an ohmmeter on each part of the film, so the conductive side will give a 0 Ω.

After the tape was stuck to the conductive side, the films were adapted into the master mold. Then the tape was cut by the two extremes parts that were not covered by the master mold using a cutter. The extreme parts are those in which FTO will be removed.

Then the etching step could be started. For that, the FTO glass prepared films were placed in a support surrounded with water, and Zn powder was poured onto the films. HCl 10% was added with a Pasteur pipette into the films covered by Zn. The Zn reacts with the acid, digesting the FTO. After some seconds the films were passed into the water to stop the digestion. If any FTO was remaining in the film, it appeared as brownish stains and we had to repeat the etching.

Once all the films were etched, the tape was removed and the films were cut in  $1.5 \times 1.5 \text{ cm}^2$ . Every square film size was checked in the evaporator mask, and the ones which did not fit the mask were discarded.

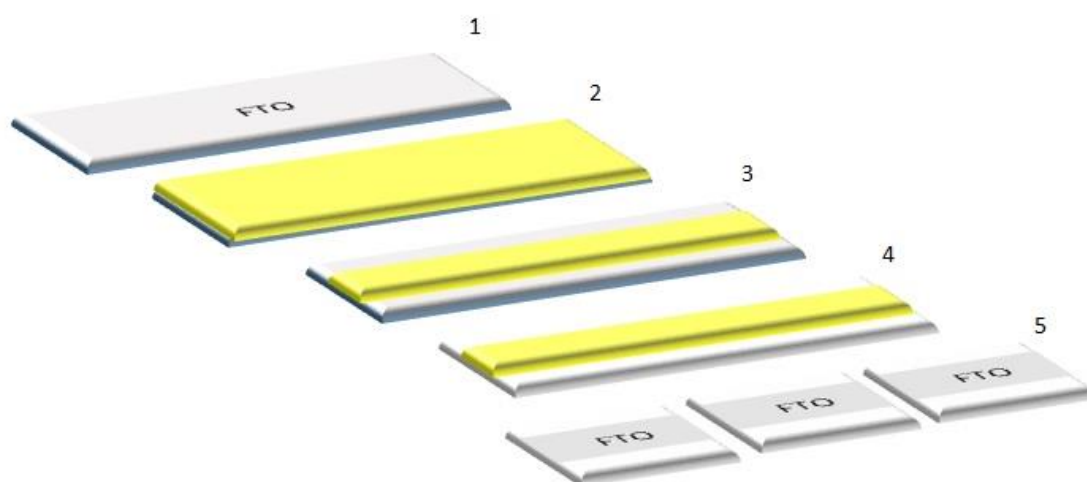


**Figure 15:** FTO glass represented in different times of the first part of device fabrication: 1) FTO glass at the beginning, 2) the film covered with adhesive tape in yellow, 3) the film with removed tape from the two extremes, which look darker, 4) the film after removing the FTO from both extremes, which now look lighter, 5) the  $1.5 \times 1.5 \text{ cm}^2$  films once removed the tape.

After the etching, the square films were marked with a diamond tip from the non-conductive side. Then they were washed with three consecutive ultrasounds baths, 10 minutes with acetone and two cycles of 10 minutes with isopropanol.

Once cleaned, a UV/ozone treatment was applied to the FTO side of the films for 20 minutes in order to remove the organic matter remaining on the surface.

After that, a compact layer of 50 nm  $\text{TiO}_2$  was deposited by spin coating in every film. The compact  $\text{TiO}_2$  solution was previously prepared mixing 0.65 ml of titanium diisopropoxide bis and 0.38 ml of Acetylacetone in 5 ml of ethanol.

After that, with a thin non-metallic tool soaked in ethanol part of the  $\text{TiO}_2$  was removed as shown in Figure :

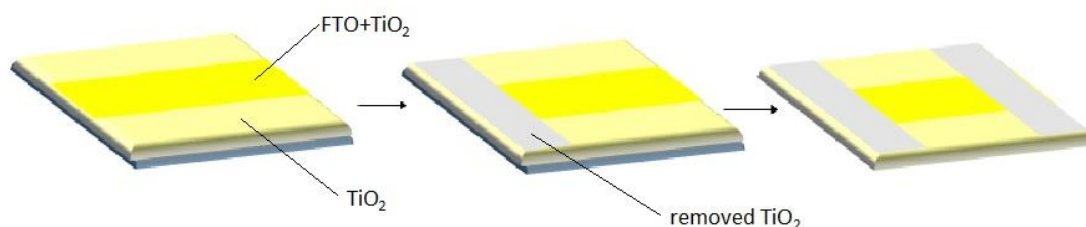


**Figure 16:** representation of the  $\text{TiO}_2$  spin-coated removed from the two extremes of every film. The dark yellow part is  $\text{FTO}+\text{TiO}_2$ , the light yellow part is  $\text{glass}+\text{TiO}_2$  and the grey part is the remaining glass when  $\text{TiO}_2$  was removed.

Once this was done for all the films, they were heated to  $500^\circ\text{C}$  for 30 minutes.

After that time, the films were cooled to room temperature and were treated in a 70 mM  $\text{TiCl}_4$  solution at  $70^\circ\text{C}$  for 30 minutes, in order to homogenize the compact  $\text{TiO}_2$  layer, which could have been irregularly deposited.

After 30 minutes, the films were washed with water and ethanol and a layer of 350 nm mesoporous  $\text{TiO}_2$  was deposited in every film by spin coating. The mesoporous  $\text{TiO}_2$  solution was previously prepared mixing  $\text{TiO}_2$  paste (18 NR-T Dyesol) and ethanol in a w:w proportion of 2:5.

After the compact layer deposition part of the m- $\text{TiO}_2$  was removed the same way as did with the compact  $\text{TiO}_2$  layer.

Then the films were heated in a hot plate with a temperature ramp with the following conditions:  $325^\circ\text{C}$  for 30 minutes;  $375^\circ\text{C}$  for 5 minutes;  $450^\circ\text{C}$  for 15 minutes and  $500^\circ\text{C}$  for 30 minutes.

While the ramp temperature was carried out, the next perovskite and HTMs solutions were prepared:

The perovskite precursor solution was prepared with 0.23 g of  $\text{PbCl}_2$  and 0.4 g of  $\text{CH}_3\text{NH}_3\text{I}$ , solving both substances through stirring at room temperature in 1 ml of N, N-dimethylformamide.

Two different HTM were used: Spiro-OMeTAD and **ML01**. The Spiro-OMeTAD precursor solution was prepared by solving 36.15 mg of commercial Spiro-OMeTAD, 14.25  $\mu\text{l}$  *tert*-butylpyridine and

8.75  $\mu\text{l}$  of lithium bis-trifluoromethanesulfonimide in 0.5 ml of chlorobenzene. The **ML01** precursor solution was prepared by solving 5 mg of the synthesized compound in 500  $\mu\text{l}$  of chlorobenzene.

Once the temperature ramp had finished and while the films were still hot, they and the three recently prepared solutions were placed inside a globe box.

There, the perovskite and the HTM solutions were filtered with a 0.2  $\mu\text{m}$  filter. Then a 100 nm layer of the filtered yellow perovskite solution was deposited on every film, over the mp-TiO<sub>2</sub> layer, by spin-coating. Gradually, as the perovskite was settling in the film, the films' colour changed from yellow to a dark orange, as seen in the Figure 17:



**Figure 17:** *the spin-coating of the perovskites into the films lasted 30 seconds. When the second film was spin-coated, the first one was already orange.*

After that, all the perovskite-coated films were left for 30 minutes, in order to evaporate the remaining solvent of the perovskite solution, and those films that did not turned orange were discarded.

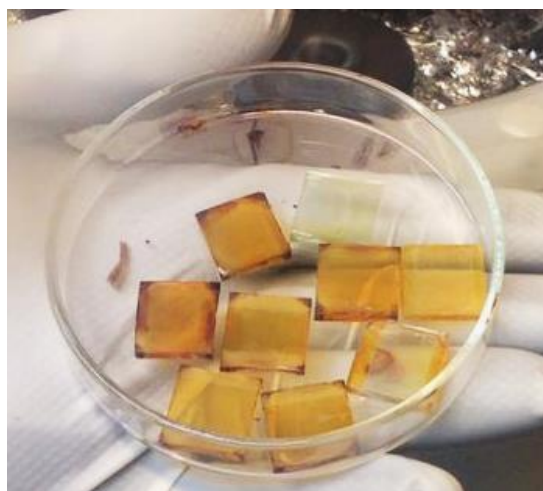


**Figure 18:** *after some perovskite spin-coatings, some films became orange and some did not. The ones which remained yellow were discarded*

The films were then heated in the hot plate at 100°C for 1 hour, and the films turned fast again to yellow at first and finally to black.

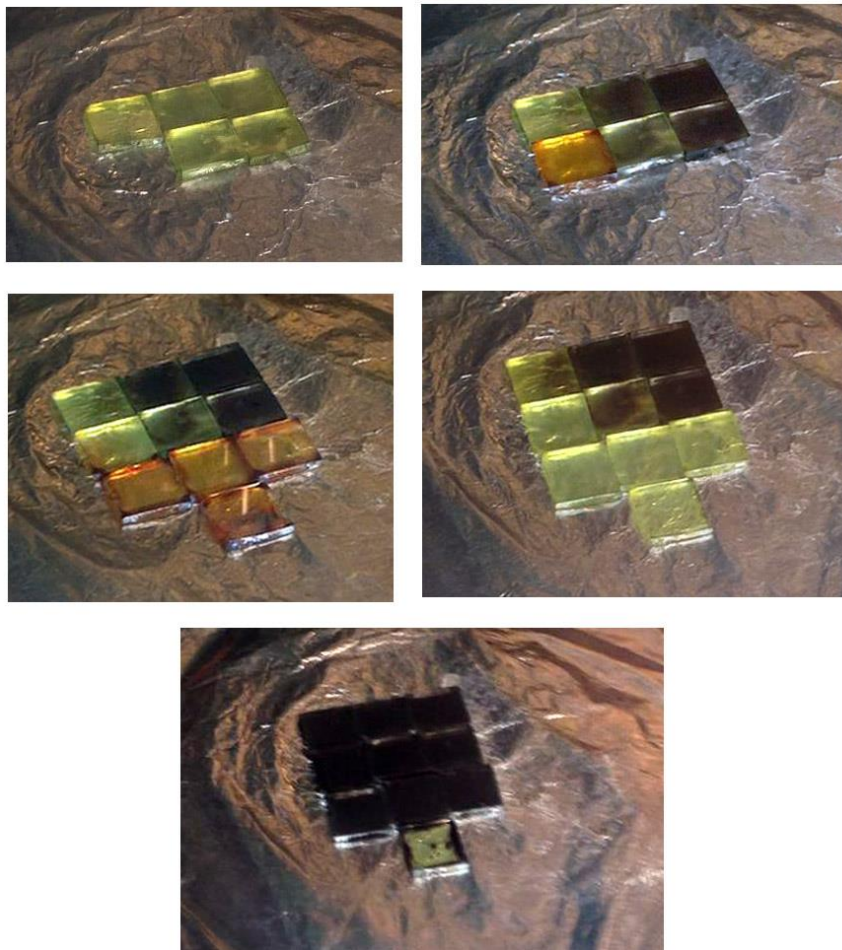


**Figure 19:** when the films were placed into the hot plate they were orange, but fast became to yellow again and finally to black, in less than 20 seconds.

After that, the 9 remaining films were separated in two groups: 4 for the Spiro-OMeTAD and 5 for **ML01**. A 100 nm of HTM layer was applied in its corresponding films the same way as did before with the perovskite layer.

After every spin-coating, the films were etched the same way and side as did for the TiO<sub>2</sub>, with a non-metallic tool soaked in DMF. The tool must be moist instead of wet, in order to avoid the dissolution of any layer in the working region of the device.

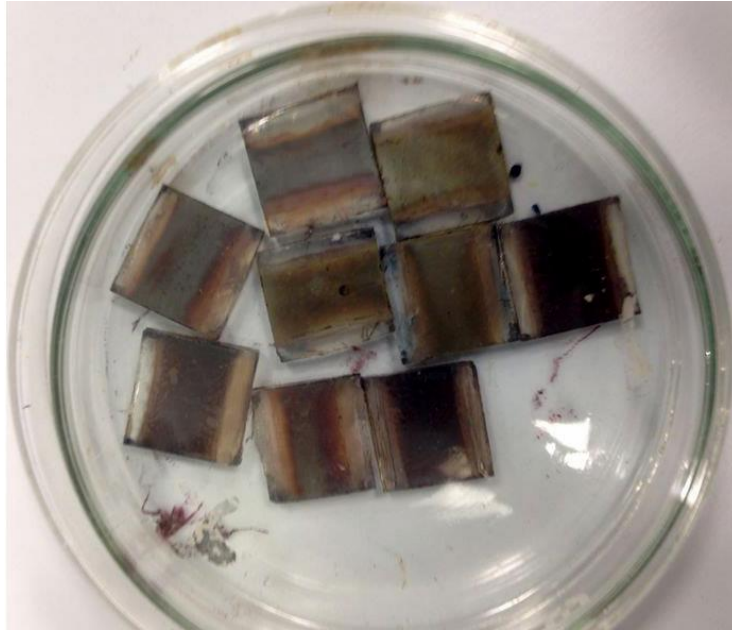


**Figure 20:** the films with all the layers except the last one (gold).

Finally, the films were placed beneath the evaporation mask and were moved inside the high vacuum thermal evaporator, where an 80 nm of a gold layer was evaporated to the films.

#### 4. Device Characterization

Devices characterization was performed using a Sun 2000 Solar Simulator (150 W), with AM 1.5 sunlight spectrum and a temperature of 25°C. The illumination intensity was measured to be 100 mW/cm<sup>2</sup> with a calibrated silicon photodiode.

Current and voltage measures were obtained and processed with Excel. The I-V curves were plotted with the same programme.

## Results and discussion

### 1. Synthesis of ML01

#### 1.1. Synthesis of 4-(*p*-tolyl)-1,2,3,4-tetrahydrocyclopenta[*b*]indole

The first reaction resulted in 0.15g of 4-(*p*-tolyl)-1,2,3,4-tetrahydrocyclopenta[*b*]indole (product **1**), as a yellow oil. Thus the first step had a very low yield of 5.32%.

The  $^1\text{H}$ -RMN spectrum expected for the product **1** presents 10 signals, corresponding to 10 anisochronous protons, represented in the next figure:

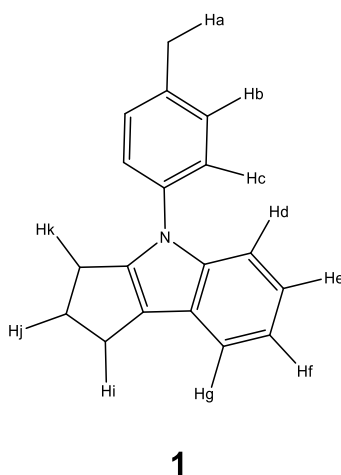


**Figure 21:** all the anisochronous protons from product **1** (4-(*p*-tolyl)-1,2,3,4-tetrahydrocyclopenta[*b*]indole)

Among these 10 signals, the most representative ones and those which will be used to identify the molecule are the aromatic ones (Hb, Hc, Hd, He, Hf i Hg), because in the aliphatic zone (Ha, Hi, Hj and Hk) signals of grass or water can be found.

The result of  $^1\text{H}$ -NMR (500 MHz,  $\text{CDCl}_3$ ) spectrum is shown in the next figure:

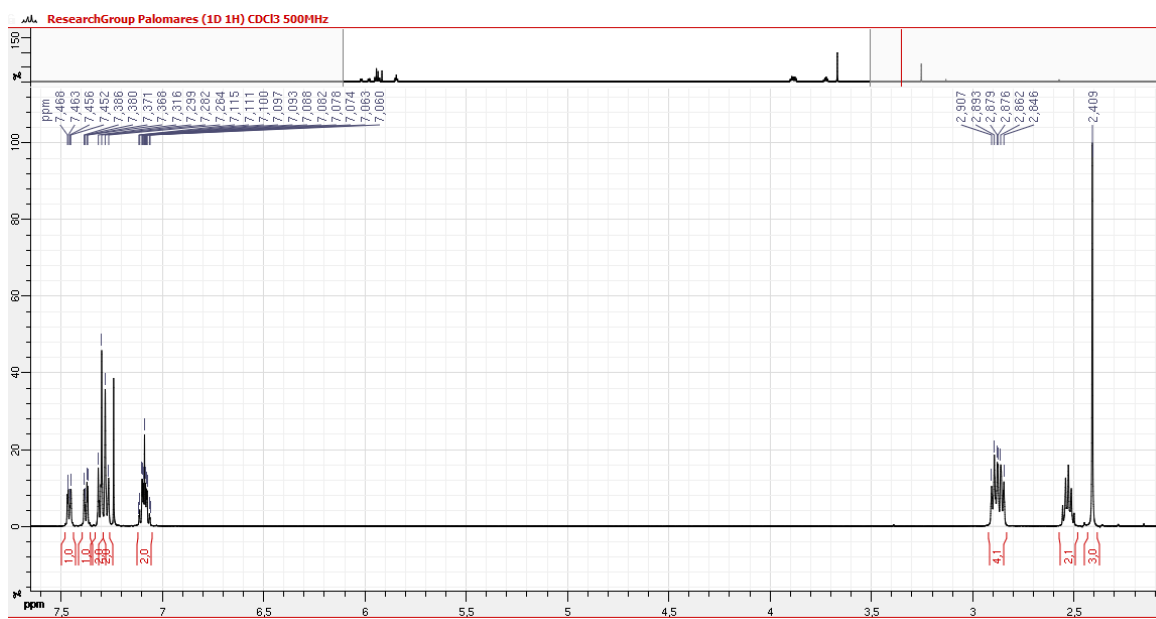


**Figure 22:** 500 MHz  $^1\text{H}$ -RMN spectra obtained from product **1** once purified, recorded in  $\text{CDCl}_3$

As shown in the spectrum, the 10 expected signals appear clearly, apart from the reference signal of the  $\text{CDCl}_3$  at 7.24 ppm, and were: 7.46 ppm (m, 1H); 7.37 ppm (m, 1H); 7.27 ppm (m, 2H); 7.09 ppm (m, 2H); 2.87 ppm (m, 4H); 2.53 ppm (m, 2H); 2.41 ppm (s, 3H).

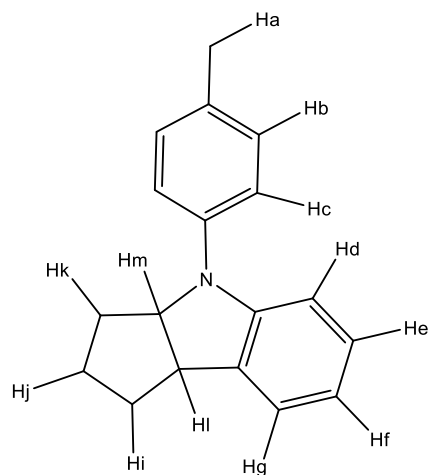
Choosing the integration reference as the 3 protons integrated by the aliphatic singlet, which corresponds to protons Ha, it is possible to obtain the integration of all the other signals.

Thus, the desired product was formed and the synthesis could proceed.

### 1. 2. Synthesis of 4-(*p*-tolyl)-1,2,3,3a,4,8b-hexahydrocyclopenta[*b*]indole

The second reaction resulted in 0.088 g of 4-(*p*-tolyl)-1,2,3,3a,4,8b-hexahydrocyclopenta[*b*]indole (product **2**), as a yellow oil. Thus the second step had a quite high yield of 89%.

The  $^1\text{H}$ -RMN spectrum expected for the product **2** presents 12 signals, 10 of them will be the same as for the product **1**, and the 2 new (Hl, Hm) are typical signals of indole compounds, which appear between 5-3 ppm, so they will be clearly differentiated.



2

**Figure 23:** all the anisochronous protons from product **2** ( 4-(p-tolyl)-1,2,3,3a,4,8b-hexahydrocyclopenta[b]indole ).

The result of  $^1\text{H-NMR}$  (400 MHz,  $\text{CDCl}_3$ ) spectrum is shown in the next figure:

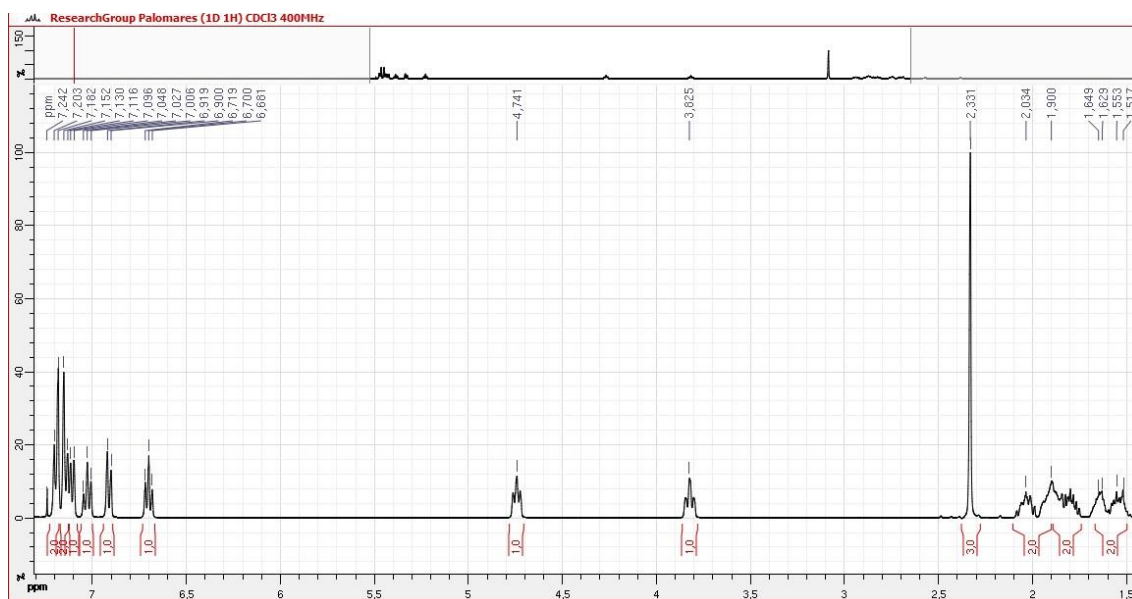


**Figure 24 :**  $^1\text{H-NMR}$  spectra obtained from product **2** once purified

As shown in the spectrum, the 10 signals from the previous molecule appear again, but also the 2 new signals expected. Taking as a reference the  $\text{CDCl}_3$  signal at 7.24 ppm, the signals obtained were: 7.19 ppm (m, 2H); 7.15 ppm (m, 2H); 7.10 ppm (d, 1H); 7.03 ppm (t, 1H); 6.91 ppm (d, 1H); 6.70 ppm (t, 1H); 4.74 ppm (m, 1H); 3.82 ppm (m, 1H); 2.32 ppm (s, 3H); 2.01 ppm (m, 2H); 1.81 ppm (m, 2H); 1.58 ppm (m, 2H).

Again, the product was formed and the synthesis could proceed.

### 1. 3. Synthesis of 7-bromo-4-(p-tolyl)-1,2,3,3a,4,8b-hexahydrocyclopenta[b]indol

The third reaction resulted in 0.141 g of 7-bromo-4-(p-tolyl)-1,2,3,3a,4,8b-hexahydrocyclopenta[b]indol (product **3**), as a white solid. Thus, the third step had yield of 23%.

This time, the  $^1\text{H}$ -RMN spectrum expected for the product **3** presents 11 signals, which are those obtained in the previous product spectrum less one, Hf, which if the reaction is successful will be substituted for a bromine.

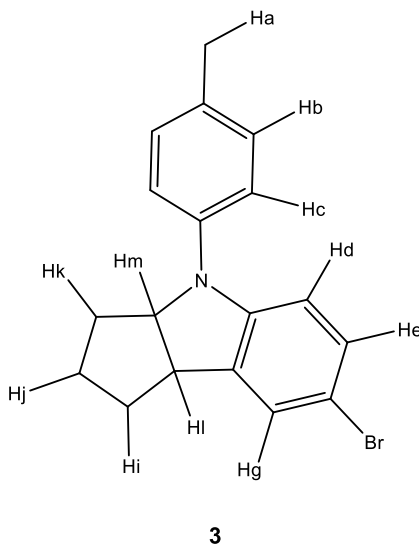


**Figure 25:** all the anisochronous protons from product **3** (7-bromo-4-(p-tolyl)-1,2,3,3a,4,8b-hexahydrocyclopenta[b]indol

The result of  $^1\text{H}$ -NMR (300 MHz,  $\text{CDCl}_3$ ) spectrum is shown in the next figure:

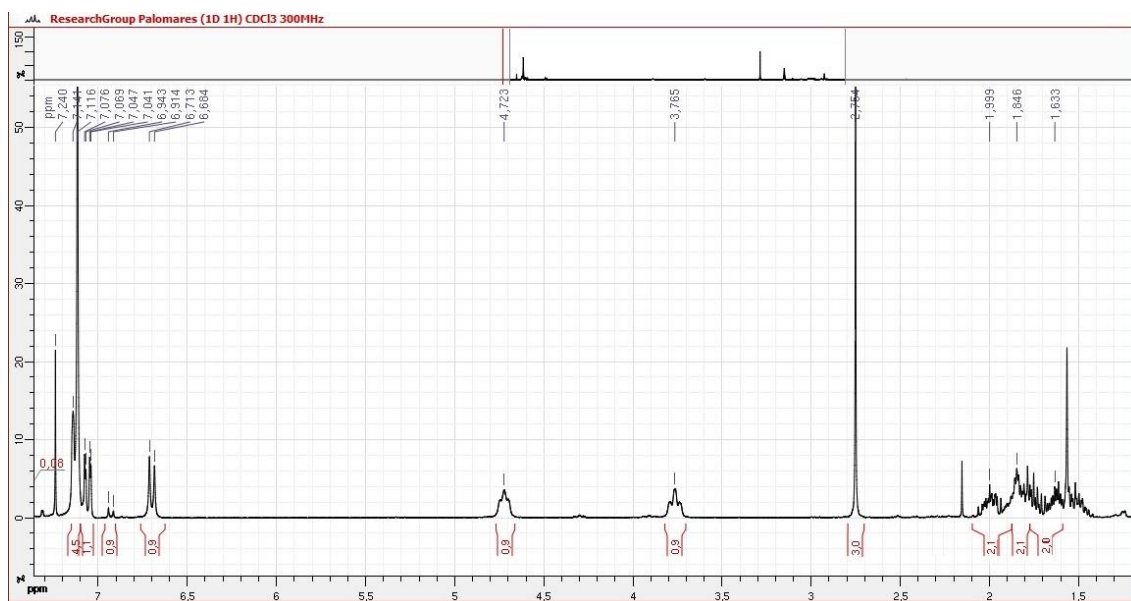


**Figure 26:**  $^1\text{H}$ -RMN spectra obtained from product **3** once purified

As shown in the spectrum, one aromatic signal was lost due to its substitution for bromine. Besides, as a result of lower resolution equipment used this time, signals had not as good resolution as the other spectra, and the first two signals appear overlapped.

Taking as a reference the  $\text{CDCl}_3$  signal at 7.24 ppm, the signals obtained were: 7.13 ppm (d, 4H); 7.06 ppm (d, 1H); 6.93 ppm (d, 1H); 6.69 ppm (d, 1H); 4.72 ppm (t, 1H); 3.76 ppm (t, 1H); 2.78 ppm (s, 3H); 1.98 ppm (m, 2H); 1.81 ppm (m, 2H); 1.68 ppm (m, 2H).

With that spectrum the obtention of the product 3 was verified and the synthesis could go on.

#### 1. 4. Synthesis of 7-(4,4,5,5-tetramethyl-1,3,2-dioxaborolan-2-yl)-4-(p-tolyl)-1,2,3,3a,4,8b-hexahydrocyclopenta[b]indole

In the fourth reaction 0.069 g of 7-(4,4,5,5-tetramethyl-1,3,2-dioxaborolan-2-yl)-4-(p-tolyl)-1,2,3,3a,4,8b-hexahydrocyclopenta[b]indole (product 4) were obtained as yellow oil. Thus, the fourth reaction led a yield of 61%.

The  $^1\text{H}$ -RMN spectrum expected this time for the product 4 have 12 signals, 11 of them are the same as from product 2 and the new one will be a very representative singlet integrating the 12 isochronous protons from the indoline boronate.

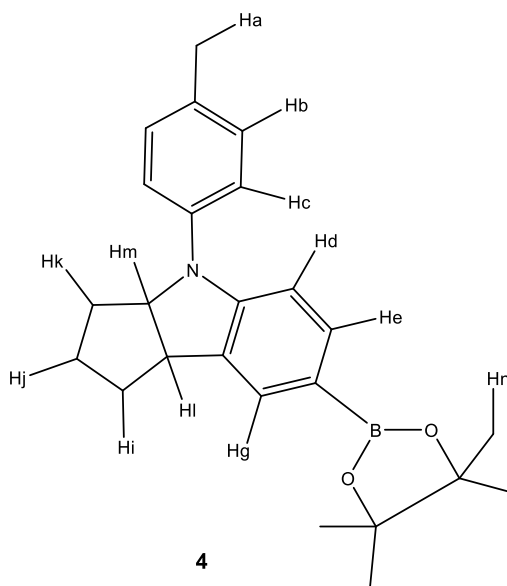


**Figure 27:** all the anisochronous protons from product 4 (7-(4,4,5,5-tetramethyl-1,3,2-dioxaborolan-2-yl)-4-(p-tolyl)-1,2,3,3a,4,8b-hexahydrocyclopenta[b]indole)

The result of  $^1\text{H-NMR}$  (400 MHz,  $\text{CDCl}_3$ ) spectrum is shown in the next figure:

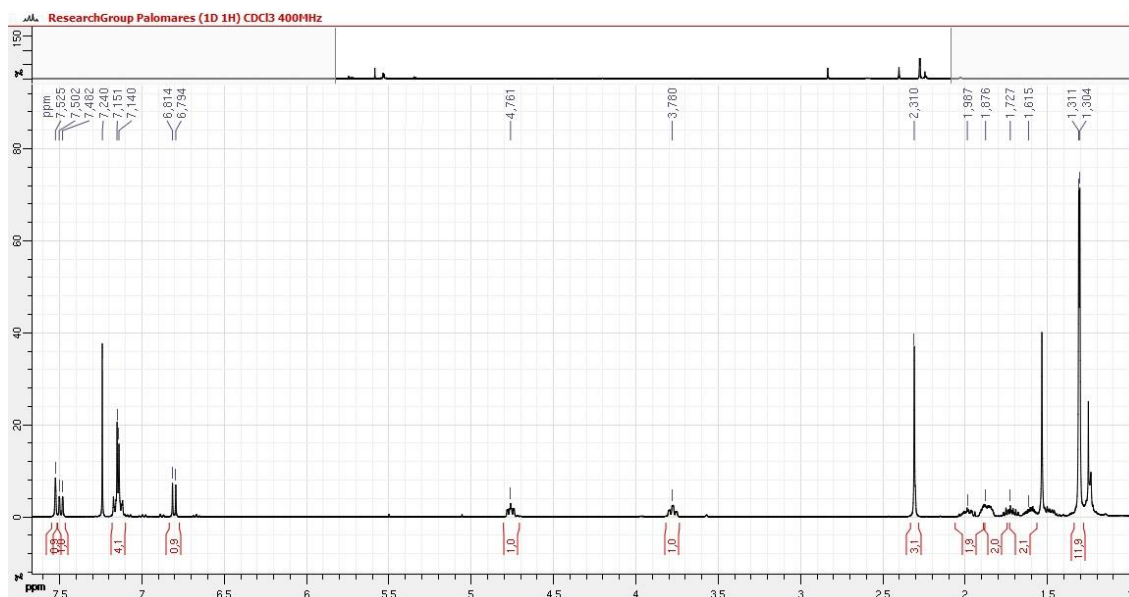


**Figure 28:**  $^1\text{H-RMN}$  spectra obtained from product **4** once purified

As shown in the spectrum, the new and more representative signal from this molecule is the singlet at 1.31 ppm that integrates the 12 H from the indoline boronate methyls. Taking the integration of these signals as the reference, it is possible to verify if the integration of the other is correct.

If the signal from  $\text{CDCl}_3$  at 7.24 ppm is taken as the reference, the signals obtained were: 7.53 ppm (s, 1H); 7.49 ppm (d,  $J=8\text{Hz}$ , 1H); 7.14 ppm (m, 4H); 6.80 ppm (d,  $J=8\text{Hz}$ , 1H); 4.76 ppm (m, 1H); 3.77 ppm (m, 1H); 2.31 ppm (s, 3H); 1.97 ppm (m, 2H); 1.82 ppm (m, 2H); 1.65 ppm (m, 2H); 1.31 ppm (s, 12H).

With these results compound **4** was identified and the synthesis could proceed.

### 1. 5. Synthesis of **ML01**:

This synthesis of **ML01** was performed two times, because the first time the desired product was not obtained.

The  $^1\text{H-RMN}$  spectrum expected for the target compound **ML01** has 12 signals, 11 of them are the same as the compound **3** and the new one is the signal given by the isochronous protons from the 4,7-dibromobenzo[*c*]-1,2,5-thiadiazole (Ho):

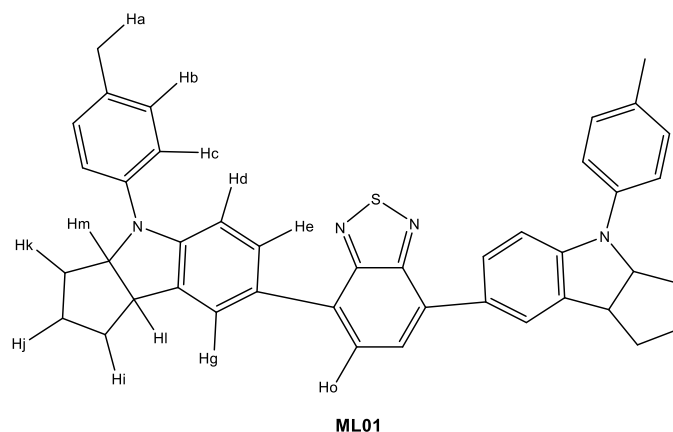


**Figure 29:** all the anisochronous protons from the target molecule **ML01**

The result of the  $^1\text{H-NMR}$  (500 MHz,  $\text{CDCl}_3$ ) spectrum done with the first red product obtained are shown in the next figure:

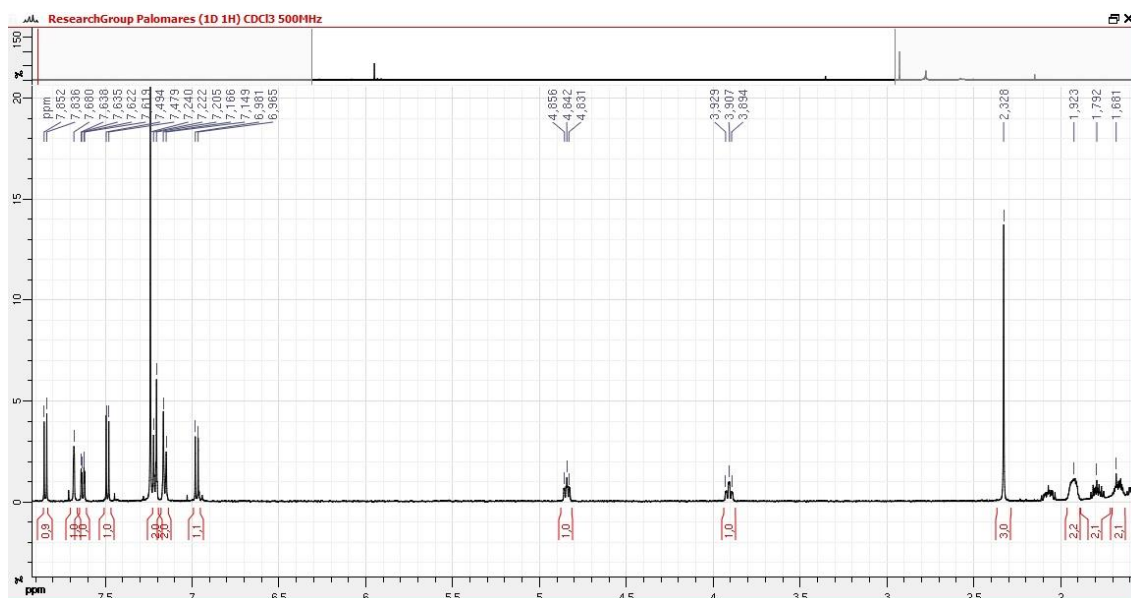


**Figure 30:**  $^1\text{H-NMR}$  spectra obtained from product **5** once purified

As shown in the spectrum, 13 signals were obtained instead of 12, and two new signals appeared in the aromatic region. Since the product expected was **ML01**, the aliphatic singlet was first set as integrating 6 H, and the spectrum obtained had then a total of 40 H, when **ML01** is supposed to have 38. The 2 extra protons correspond to the 13<sup>th</sup> signal.

Looking for possible molecules which fit the spectrum obtained, some possible product were though. Among them, the one that fits the most with the spectrum obtained is **5**, which have the 2 anisochronous (Ho, Hp) protons from the diazothiazole part and as a result its expected spectrum presents 2 more signals in the aromatic zone. Moreover, it would explain why if the integration is doubled, the total protons obtained are 40.

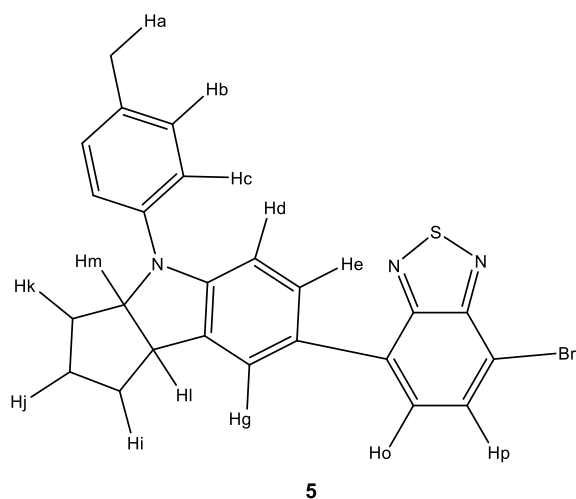


**Figure 31:** all the anisochronous protons from the molecule formed, **5**.

In order to verify if product **5** was obtained, J coupling constants were measured. Thus, if product **5** was obtained, the spectrum expected has to present 3 different J (ortho) coupling constants, one of them corresponding to Ho-Hp coupling.

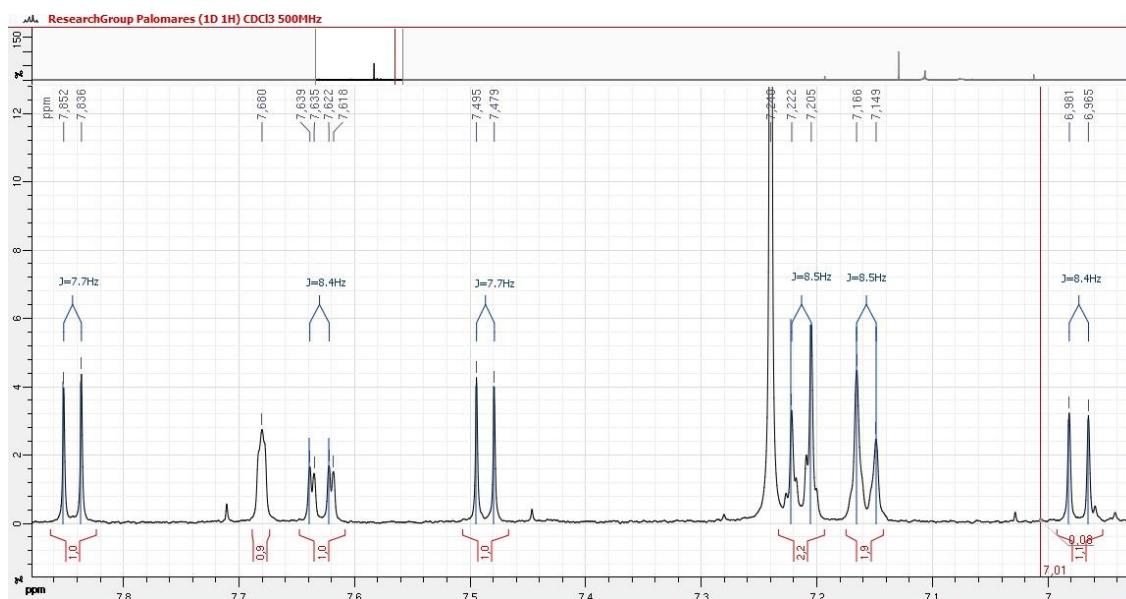


**Figure 32:** aromatic extended region from the  $^1\text{H}$ -RMN spectra obtained from product **5**.

As shown in the extended spectrum, 6 signals presented an ortho-coupling and were correlated 3 to 3: Hb-Hc, Hd-He and Ho-Hp.

Thus, product **5** was identified and the synthesis was repeated from step iv.

Finally, after the last Suzuki performance, two products were obtained. The first one was red, and the  $^1\text{H}$ -RMN spectrum obtained showed that it was product **5** again. The second one was pink, and the  $^1\text{H}$ -RMN (400 MHz,  $\text{CDCl}_3$ ) spectrum obtained is shown in the next figure:

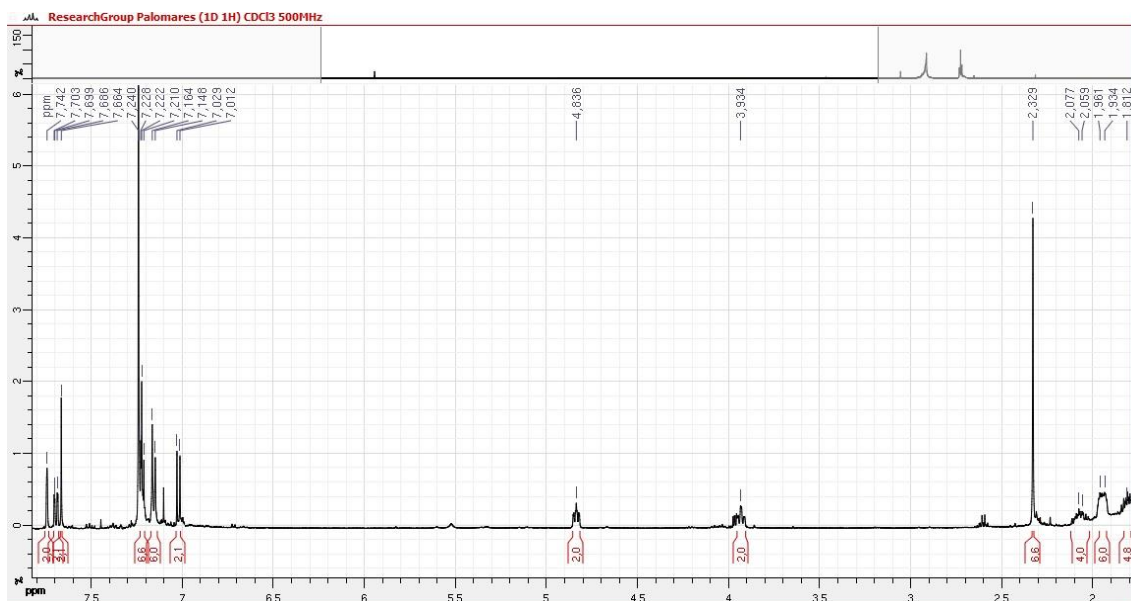


**Figure 33:**  $^1\text{H}$ -RMN spectra obtained from the pink product once purified

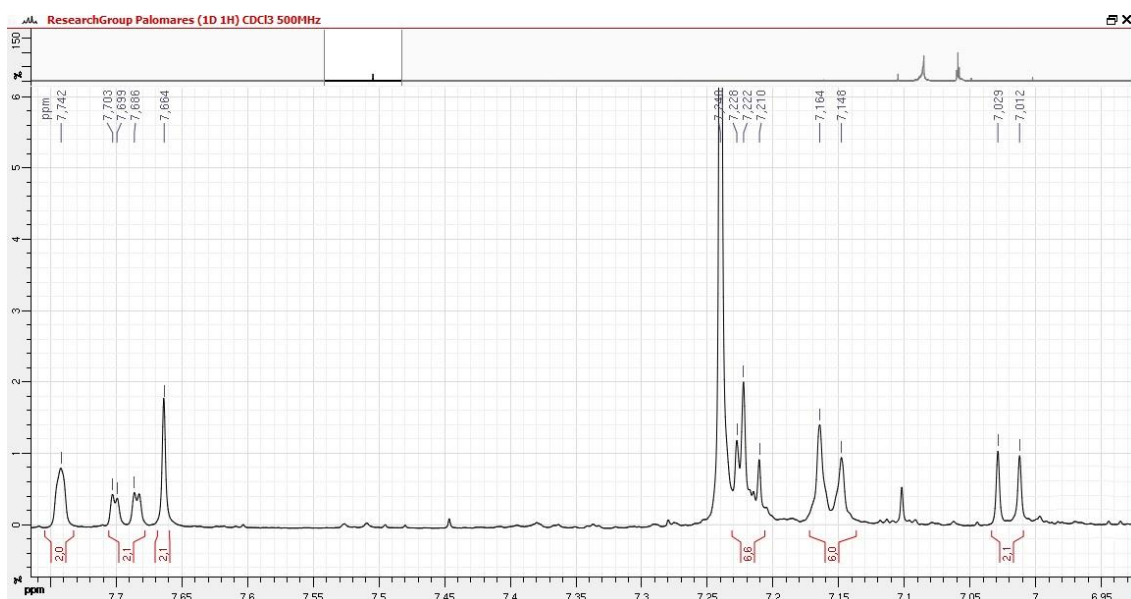


**Figure 34:** aromatic extended region from the  $^1\text{H}$ -RMN spectra obtained from the pink product once purified.

As shown in the spectrum, the 6 expected signals in the aromatic zone were obtained this time. Due to the low amount of product synthesized, the signals had low resolution and a lot of noise can be seen in the spectrum. Thus, the integration of some signals given by the programme is not correct, because it also integrates the noise.

Taking as a reference the  $\text{CDCl}_3$  signal at 7.24 ppm, the signals obtained were: 7.74 ppm (s, 2H), 7.69 ppm (dd, 2H); 7.66 ppm (s, 2H), 7.22 ppm (d, 4H), 7.15 ppm (d, 4H), 7.02 ppm (d, 2H), 4.84 ppm (t, 2H), 3.94 ppm (t, 2H), 2.33 ppm (s, 6H), 2.06 ppm (m, 4H), 1.93 ppm (m, 4H), 1.79 ppm (m, 4H).

Given these results, the obtention of the target molecule was finally verified. Unfortunately, steps iv and v of the synthesis had to be repeated, and the Suzuki precursor was not purified. Consequently, and because of a lack of time which did not allow the synthesis repetition, just 5 mg of the target compound were finally obtained, which led a very low yield of 16 %.

Although the amount of **ML01** obtained was enough for the device fabrication,  $^{13}\text{C}$ -RMN and MS, which should have been performed in order to characterize the molecule, could not be realised.

## 2. Device characterization

After all device characterization, current and voltage measures were processed with Excel.

$V_{oc}$ ,  $J_{sc}$ , MP, FF and PCE were obtained for every device using the data obtained and the formulas (1), (2), (3) and (4) of the Photovoltaic Performance section.

Figure 35 and Figure 36 show the I-V curves for the best devices obtained, in terms of PCE, containing the HTM layer one with Spiro-OMeTAD and the other **ML01**.

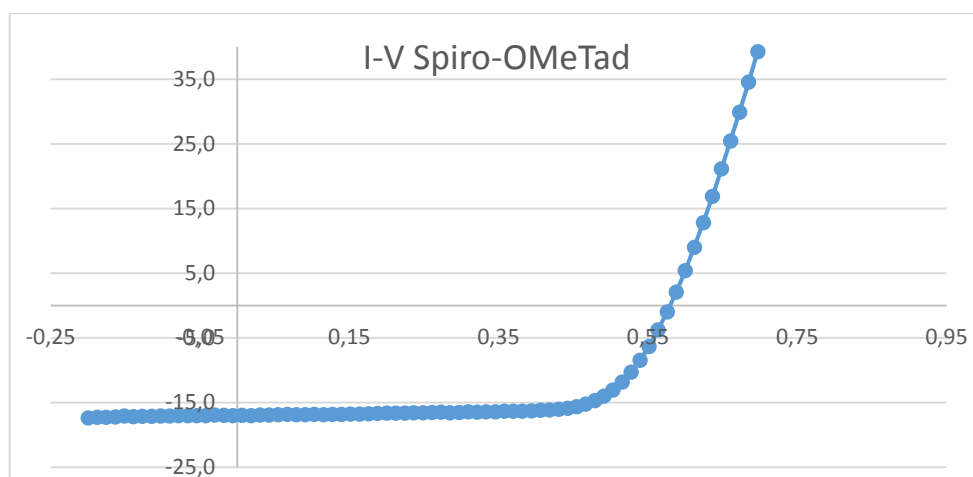


**Figure 35:** I-V curve obtained with the Spiro-OMeTAD solar cell with the highest PCE

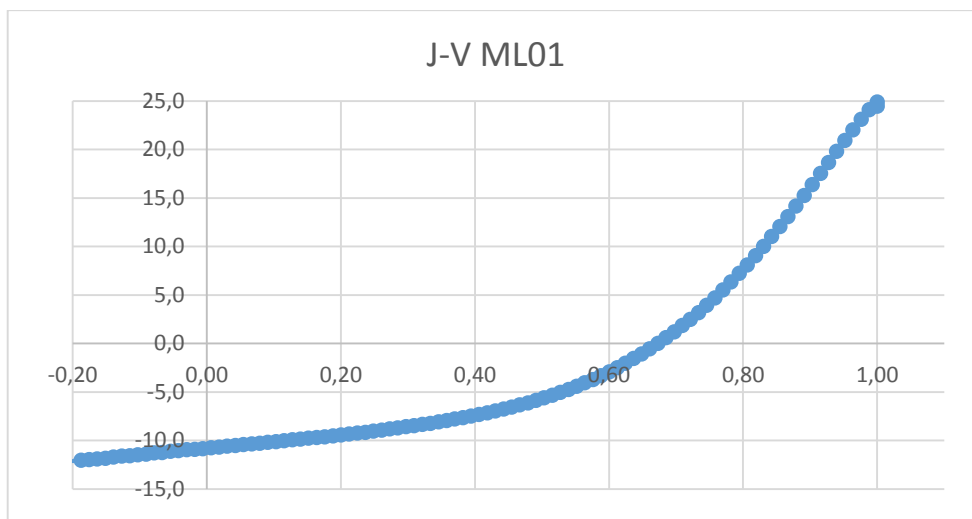


**Figure 36:** I-V curve obtained with the **ML01** solar cell with the highest PCE

The photovoltaic characteristics showed by the best 2 devices obtained using Spiro-OMeTAD and **ML01** as HTM are resumed in the next table:

**Table 2:** I-V characteristics of photovoltaic measurements

HTM	$J_{sc}$	$V_{oc}$	FF	PCE (%)
Spiro-OMeTAD	16,99	0,59	71,27	7,12
ML01	10,77	0,66	42,13	3,00

As shown in the graphics, the device with Spiro-OMeTAD as the HTM gives a much more ideal behaviour than one obtained with **ML01**, because the FF of the first curve is much squarer than the second one.

The results from Table 2 verify that not only is the FF of the first graphic much higher, because it is much closer to 100, but the maximum current that the device can generate ( $J_{sc}$ ) is also higher. On the other hand, the  $V_{oc}$  for the Spiro-OMeTAD device is smaller than that obtained with the **ML01**, meaning that this contribution to PCE is favourable for the **ML01** cell.

These results lead to a PCE of 7.12% for Spiro-OMeTAD devices, which is more than double the PCE obtained with **ML01** cells.

## Conclusions

In the present work 70 mg of the molecule **ML01** were aimed to obtain. Due to the low yields obtained for most of the steps in the synthesis and the lost of one intermediate, only 5 mg were finally synthesized. Since this amount was used to fabricate the devices, the novel molecule **ML01** could only be characterized using  $^1\text{H}$ -RMN. If a higher amount of **ML01** had been obtained a MS and a  $^{13}\text{C}$ -RMN would have been performed.

However, the amount obtained was enough to prepare a battery of cells using **ML01** as HTM. Another battery of cells were prepared with the same procedure using Spiro-OMeTAD as HTM. Both batteries of cells were characterized and the data obtained was processed. Finally the maximum PCE obtained were 7.12% for Spiro-OMeTAD cells and 3.00% for **ML01** devices.

These results do not demonstrate that **ML01** contributes to a higher PCE on perovskites solar cells, but because of the lack of experience on fabricating these devices, the low amount of devices characterized, the results are promising. Optimizing the synthesis of **ML01** and the device fabrication or even complementing the **ML01** with additives, a much higher PCE may be obtained.

## Conclusions

En aquest treball es va proposar obtenir un mínim de 70 mg de la molècula ML01 sintetitzada. A causa dels baixos rendiments obtinguts en cada pas de la síntesi, i de la pèrdua d'intermedi en un dels passos, només se'n van poder obtenir 5 mg. En conseqüència, i com que aquesta quantitat es va destinar a fabricar cel·les, de la molècula ML01, fins ara mai sintetitzada, només se'n va poder fer un espectre d' $^1\text{H}$ -RMN. En cas d'haver-ne obtingut més, s'hagués realitzat un espectre  $^{13}\text{C}$ -RMN i un espectre de masses per tal de fer una millor caracterització.

Tanmateix, es van poder preparar una sèrie de cel·les solars de perovskita amb la quantitat de ML01 obtinguda. Aquestes cel·les van caracteritzar-se juntament amb les que es van preparar amb la molècula de referència Spiro-OMeTAD amb el mateix procediment, i les dades obtingudes es van processar. Els resultats obtinguts en qüestió d'eficiència de les cel·les van ser un 7.12% amb les de Spiro-OMeTAD i un 3.00% amb les de ML01.

Aquests resultats no demostren que la molècula ML01 aporti una major eficiència a les cel·les, però tenint en compte que només es va poder fer una bateria de cel·les i davant la falta d'experiència en aquest camp, els resultats no són descoratjadors. Segurament, optimitzant la síntesi de ML01 o afegint additius en la preparació de la capa per la cel·la solar, es puguin obtenir resultats molt majors.

## Bibliography

1. <http://pureenergies.com/us/blog/the-advantages-of-solar-power-vs-other-renewable-energy-sources/> (18/12/2014)
2. Office of Energy & Renewable Energy US. [https://www1.eere.energy.gov/solar/pdfs/solar\\_timeline.pdf](https://www1.eere.energy.gov/solar/pdfs/solar_timeline.pdf) (03/01/2015)
3. Green, M.A.; Emery, K.; Hishikawa, Y.; Warta, W.; Dunlop, E. D.; Solar cell efficiency tables (version 44). *Prog. Photovolt*, **2014**, *22*, 701-710.
4. Moon, S-J., Solid-State Sensitized Heterojunction Solar Cells: Effect of Sensitizing Systems on Performance and Stability, PhD thesis, École Polytechnique Fédérale de Lausanne (2011).
5. Park, N-G.; Perovskite solar cells: an emerging photovoltaic technology. *Mater. Today*. **2014**, DOI: 10.1016/j.mattod.2014.07.007
6. Jutglar, L.; Sistemas Fotovoltaicos (FV). In *Energía Solar*. Ediciones CEAC; Planeta deAgostini Profesional y Formación, S. L.: Barcelona, 2004, 155-187.
7. Kojima, A.; Teshima, K.; Shirai, Y.; Miyasaka, T. Organometal Halide Perovskites as Visible-Light Sensitizers for Photovoltaic Cells. *J. Am. Chem. Soc.* **2009**. *131*, 6050-6051.
8. Liu, M.; Johnston, M. B.; Snaith, H. J. Efficient planar heterojunction perovskite solar cells by vapour deposition. *Nature*. **2013**. *501*. 395-398.
9. Mishra, A.; Bäurle, P.; Small Molecule Organic Semiconductors on the Move: Promises for future Solar Energy Technology. *Angw. Chem. Int.* **2012**. *51*. 2020-2067.
10. PVEducation.org. <http://pveducation.org/pvcdrom/solar-cell-operation/efficiency> (27/12/2014)
11. Howie, W. H.; Claeysens, F.; Miura, H.; Peter, L. M. Characterization of Solid-State Dye-Sensitized Solar Cells Utilizing High Absorption Coefficient Metal-Free Organic Dyes. *J. Am. Chem. Soc.* **2008**. *130*. 1367-1375.
12. Sigma-Aldrich. <https://www.sigmaaldrich.com/spain.html> (02/01/2015)